Politecnico di Torino
Dipartimento di Elettronica e delle Telecomunicazioni

Corso di Laurea Magistrale in Nanotechnologies for ICTs

Tesi di Laurea Magistrale

Homotopy analysis method for non linear MEMS resonators

Candidato
Giulio de Vito
Matricola 245731

Relatore
Carlo Ricciardi

Anno Accademico 2018–2019

ABSTRACT

In this thesis an algorithmic procedure to characterize a non linear harmonic resonator is described and the computation of the resonator's stability limit potential is performed by the means of homotopy analysis method. The homotopic amplitude response approximation is reduced to a third order polynomial using Cardano's formulae. With the extracted solutions, a batch of mock data is generated. Consequently, the mock data is fitted to check its sensitivity to initial conditions and the formula is used to fit experimental data.
Python is used as the coding language to perform all operations and the code is disclosed. The summary of the algorithm's robustness and the fitting of the experimental data are reported, the setup used is also described. The experiments were carried out with industrial pressure sensors of microGauge AG. The results obtained proves that the following method can be used to characterize non linear oscillator for industrial applications.

CONTENTS

1 INTRODUCTION 1

2 NON LINEAR HARMONIC RESONATOR 3
- 2.1 Duffing equation 3
- 2.2 H.A.M applied to resonator 5
- 2.3 H.A.M. solution 6
- 2.4 Cardano's method 7

3 METHODOLOGY 11
- 3.1 Mock data 11
- 3.2 Parameters analysis 14
- 3.3 Fitting 19
  - 3.3.1 Fitting mock data 19
  - 3.3.2 Fitting results 23
- 3.4 Fitting experimental data 31
  - 3.4.1 Set-up 31
  - 3.4.2 Fitting of the experimental data 34

4 RESULTS AND DISCUSSION 38
- 4.1 Linearity's boundary identification 38
- 4.2 Limit potential 39

5 CONCLUSION 42

A H.A.M.: MATHEMATICS 43
- A.1 Duffing equation 43
- A.2 H.A.M. convergence 46
- A.3 Higher-order deformation equation 48
- A.4 First order H.A.M approximation 48
- A.5 Straight beam with double clamped electrodes 49

B MICROGAUGE PROFITS 51

List of Symbols 53

BIBLIOGRAPHY 56

LIST OF FIGURES

Figure 2.1 Potential $V(u)$ 5
Figure 3.1 Mock data 14
Figure 3.2 Delta positivity 16
Figure 3.3 k_3 variation 17
Figure 3.4 μ variation 18
Figure 3.5 K variation 19
Figure 3.6 Example of fitted mock data 24
Figure 3.7 Example of not fitted mock data 26
Figure 3.8 k_3 extracted for $\mu_{estimated} = 0.0001$ 27
Figure 3.9 k_3 extracted for $\mu_{estimated} = 0.001$ 28
Figure 3.10 k_3 extracted for $\mu_{estimated} = 0.01$ 29
Figure 3.11 Experimental set-up 32
Figure 3.12 Sensor schematic 33
Figure 3.13 Lorentzian fit 35
Figure 3.14 Experimental fitting 36
Figure 3.15 k_3 extraction summary 37
Figure 4.1 Bistable resonator 39
Figure 4.2 Linearity limit 41
Figure A.1 Hardening and Softening behaviour of Duffing resonator 44
Figure A.2 Non linear spring 45
Figure A.3 Straight beam 49

1 INTRODUCTION

AIM

The company microGauge is a start-up and spin off of E.T.H. (Swiss Federal Institute of Technology), that develops pressure sensors. Every new sensor needs to be calibrated before being used. An operator performs several frequency sweeps with different actuation potentials and the response amplitude is evaluated. The operator chooses the actuation potential that makes the oscillator look linear.
This procedure aims to find the best signal to noise ratio, since every sensor has lower detection limit due to electronics noise, the input signal needs to be amplified up to the linearity boundary. However, the company used to make those measurements manually trying different actuations, then by evaluating the response, the actuation potential that make the response's amplitude look like a Cauchy distribution is choosen. This kind of procedure depends on the arbitrary evaluation of the operator so, to make the calibration automatic, an algorithm to find an objective set-point is necessary.
The aim of this porject is to find an objective set-point, for an automatic calibration procedure of pressure sensors.

H.A.M.: HOMOTOPY ANALYSIS METHOD

Shijun Liao, the author of homotopy analysis method, describes the homotopy analysis as "a global convergent numerical method mainly for non linear differential equations" [1, Advances in the homotopy analysis method, page v].
The roots of this method reside in the concept of homotopy, which consists of the continuous transformation of one function to another, especially mapping space "MAP(X, Y)" from the first function to the second. Two mathematical objects are said to be homotopic if one can be continuously deformed into the other, this concept was first formulated by Poincaré around 1900 [2, Homotopy Theory and Models].
An example of homotopy can be a continuous deformation of a cup to a doughnut shape. However, the cup cannot be continuously deformed into a sphere because this kind of shape does not contain an opening.
In the frame of non linear analytic solutions, the novelty of H.A.M. consists of:

1. no dependence on small physical parameters
2. great freedom to choose the analytic equation and solution expression of high order approximation

3. guaranteeing the convergence of approximation series

[1, Advances in the homotopy analysis method, page 5]
Georg Cantor pointed out in his book [3, From Kant to Hilbert : a source book in the foundations of mathematics] that "the essence of mathematics lies entirely in its freedom". This quote resumes fully the substance of H.A.M.
The flexibility of choosing the equation type and the solution expression are the keys of the success of H.A.M. Some noticeable examples of the achievements of this method are listed below:

- boundary-layer flows
- optimal boundary of American put option
- multiple equilibrium-states of resonant waves in deep water

Other examples can be found in [1, Advances in the homotopy analysis method].
In this thesis, H.A.M. is applied to study the non linear regime of a harmonic resonator and the non linear factor is correlated with the actuation potential of the resonator.
H.A.M. provides a powerful solution to predict the amplitude response in strongly non linear oscillator, conversely it can parse significant parameters from the experimental data of a resonator as described in chapter 2. Chapter 3 illustrates the methodology used, with examples of mock and experimental data, and chapter 4 discusses how to employ the results in the frame of automatic calibration.
The mathematical assumption and correlation are in the Appendix A or in the paper [4, Nonlinear dynamics of MEMS/NEMS resonators]. In the Appendix B the company's gain from this project is presented and in the Appendix B the list of symbols used is shown.

2 NON LINEAR HARMONIC RESONATOR

Starting from the linear harmonic oscillator, non linear resonator behaviour is discussed with a description of its potential function.
A brief explanation on how to use homotopy analysis method to extrapolate non linear solutions is provided and using Cardano's formulae an explicit solution is extracted.

2.1 DUFFING EQUATION

The Duffing equation was developed by Georg Duffing during the first world war at the Technical University of Berlin.

$$\frac{\mathrm{d}^2u}{\mathrm{d}\tau^2} + \mu \cdot \frac{\mathrm{d}u}{\mathrm{d}\tau} + \lambda^2 \cdot u + k_2 \cdot u^2 + k_3 \cdot u^3 = K \cdot \cos(w \cdot \tau) \tag{2.1}$$

The expression 2.1 is a non linear second order differential equation where:

- $u(\tau)$: modal displacement
- τ : time
- μ : viscous damping
- λ : natural frequency of the beam in its equilibrium configuration
- w : actuation frequency
- K : actuation amplitude
- k_2 : second order non linear term
- k_3 : third order non linear term

This equation became well-known to study different phenomena, from non Hooke springs to electronic circuits and transformers with iron core. In particular the k_2 coefficient represents the long-term mean displacement of the resonator that presents a static buckling, while the k_3 parameter represents the third order coefficient of a non linear Hooke's spring:

$$F = C_1 z + C_3 z^3$$

Where F is the force applied, C_1 the linear spring constant, C_3 the first order approximation term of the non linear spring constant and z the displacement.

The appearance of $C_3 z^3$ leads the resonator to have hardening or softening effect, further details in A.1b.
The linear correspond of the Duffing equation is the *harmonic oscillator* [5, The Duffing oscillator].

$$\frac{d^2u}{d\tau^2} + \mu \cdot \frac{du}{d\tau} + \lambda^2 \cdot u = K \cdot \cos(w \cdot \tau) \tag{2.2}$$

The linear configuration of a resonator can be solved analytically and can be a starting point to study the non linear case. The solution is:

$$u(\tau) = K \cdot \cos(w\tau - \varrho) \tag{2.3}$$

Which inserted into the oscillator gives an ellipse in the phase space $(x, v) = (x, \dot{x})$ [5, The Duffing oscillator, page 158].

$$\left(\frac{u(\tau)}{K}\right) + \left(\frac{\dot{u}(\tau)}{wK}\right) = 1 \tag{2.4}$$

The amplitude u and the phase shift ϱ depend on the driving frequency w, which shows a behaviour similar to a Lorentzian function:

$$u(w, A, \lambda, \sigma) = \frac{A}{\pi} \frac{\sigma}{(w^2 - \lambda^2) + \sigma^2} \tag{2.5}$$

$$\tan(\varrho(w)) = \frac{\mu \cdot w}{\lambda^2 - w^2} \tag{2.6}$$

In which σ is the standard deviation of the Lorentzian function.
The resonance frequency is [5, The Duffing oscillator, page 158]:

$$w_{res} = \sqrt{\lambda^2 - (\mu/2)^2} \tag{2.7}$$

The appearance of the cubic term in the non linear formula introduces complexity into the solution, in particular the superposition principle is no longer valid so the linear combination of orthogonal solutions does not solve the equation of the motion.
The long time behaviour trajectories approach different types of strange attractors for diverse initial conditions. Several strange attractors can also coexist in the same phase plane. More information can be obtained by parsing the potential belonging to the time independent part of the force:
integrating the segment $\lambda^2 \cdot u + k_3 \cdot u^3$, an approximation of the potential $V(u)$ is obtained. This equation shows an heuristic behaviour of the real potential.

$$V(u) = \frac{1}{2}\lambda^2 \cdot u^2 + \frac{1}{4}k_3 \cdot u^4 \tag{2.8}$$

The equation 2.8 can be viewed as the Taylor expansion of a general, symmetric, potential [5, The Duffing oscillator, page 159]. An important factor is the parameter λ^2 that can also be negative, in the latter case λ cannot be considered as a frequency. The figure 2.1 shows the potential function for the cases λ^2 positive and negative. For u close to zero the potential is almost harmonic while for $\lambda^2 < 0$ the system shows two local minima at:

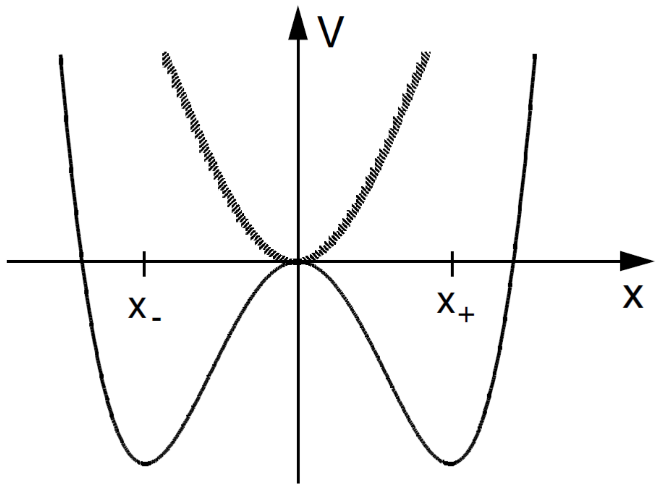

Figure 2.1: Potential function in case of a positive λ^2 (thin line) and negative λ^2 (thick line). This image was extracted from the article [5, The Duffing oscillator, page 159]

$$u_{\pm} = \pm\sqrt{-\lambda^2/k_3} \tag{2.9}$$

with depth $-\lambda^4/4k_3$.
The two local minima can explain the hysteresis behaviour of certain oscillator, however the problem's complexity requires an exhaustive mathematical analysis.

2.2 H.A.M APPLIED TO RESONATOR

An analytical solution which is able to predict the non-linear response of a mechanical resonator is also capable of predicting a hardening-type behaviour, softening-type or mixed frequency response. It starts with the definition of "rule of the solution expression" which consists of an equation responsible for computing the deviation in temporal average of amplitude [4, Non linear dynamics of MEMS/NEMS resonators]. It is supposed that the solution of equation 2.1 is the following:

$$u(\tau) = \delta + \sum_{k=1}^{\infty} \left(U_k \cdot \exp(ikw\tau) + \overline{U}_k \cdot \exp(-ikw\tau)\right) \tag{2.10}$$

- δ: long-time average of the harmonic response
- U_k, $\overline{U}_k$: complex conjugate constants

Using an embedded parameter $p \in [0, 1]$ it is possible to exhibit a continuous evolution from an initial estimation to the exact solution. More details are reported in the Appendix A.
The zero-order deformation equation is stated below A.11:

$$(1 - p) \cdot \Gamma [\phi (\tau, p) - u_0(\tau)] = c_0 \cdot p \cdot \Psi [\phi (\tau, p)] \tag{2.11}$$

The expression 2.11 represents the starting point for the deformation equation of higher order equations.
Given $u_0(\tau)$ as the initial estimate using the template of eq. A.12, the first order deformation equation is displayed in A.19:

$$\frac{\partial^2 u_1(\tau)}{\partial \tau^2} + w^2 \cdot u_1(\tau) = c_0 \cdot \Psi [u_0 (\tau), \tau] \tag{2.12}$$

The formula A.19 must have bounded solution so it is necessary to eliminate the secular and constant terms by setting them to zero.
Zeroing secular terms:

$$c_0 \cdot f_1 \left(U, \overline{U}, \delta\right) = 0 \tag{2.13}$$

Zeroing constant terms:

$$c_0 \cdot g_1 \left(U, \overline{U}, \delta\right) = 0 \tag{2.14}$$

The coefficients U, $\overline{U}$ are defined by the amplitude z and the phase shift b of the response signal.

$$\begin{aligned} U &= \frac{1}{2} z e^{i \cdot b} \\ \overline{U} &= \frac{1}{2} z e^{-i \cdot b} \end{aligned} \tag{2.15}$$

Introducing them into equations A.20 and A.21, it is possible to obtain the long-time average constant and the response frequency.

$$\delta = \frac{-z^2 \cdot k_2}{2\lambda^2 + 3z^2 \cdot k_3} \tag{2.16}$$

$$\left(2k_2 \cdot \delta \cdot z + \frac{3}{4} k_3 \cdot z^3 + \left(\lambda^2 - w^2\right) \cdot z\right)^2 + (\mu \cdot w \cdot z)^2 = K^2 \tag{2.17}$$

2.3 H.A.M. SOLUTION

In the case where the steady state average of the system response is zero, then $\delta = 0$. So, the first order solution is:

$$\left(\frac{3}{4} k_3 \cdot z^3 + \left(\lambda^2 - w^2\right) \cdot z\right)^2 + (\mu \cdot w \cdot z)^2 = K^2 \tag{2.18}$$

The quadratic term is now expanded:

$$\frac{9}{16}k_3^2 \cdot z^6 + \frac{3}{2}k_3\left(\lambda^2 - w^2\right) \cdot z^4 + \left[\mu_0^2 \cdot w^2 + \left(\lambda^2 - w^2\right)^2\right] \cdot z^2 = K^2 \tag{2.19}$$

With the replacement of $y = z^2$ it is possible to solve the above equation as a third-order polynomial, losing three of the six solutions. Since the equation is even, the six solutions are symmetrical and solving the third order equation gives the positive portion of the solutions.

$$\frac{9}{16}k_3^2 \cdot y^3 + \frac{3}{2}k_3\left(\lambda^2 - w^2\right) \cdot y^2 + \left[\mu_0^2 \cdot w^2 + \left(\lambda^2 - w^2\right)^2\right] \cdot y - K^2 = 0 \tag{2.20}$$

The coefficients are substituted for clarity.

$$a = \frac{9}{16}k_3^2 \tag{2.21}$$

$$b = \frac{3}{2}k_3\left(\lambda^2 - w^2\right) \tag{2.22}$$

$$c = \left[\mu_0^2 \cdot w^2 + \left(\lambda^2 - w^2\right)^2\right] \tag{2.23}$$

$$d = -K^2 \tag{2.24}$$

$$\tag{2.25}$$

It yields:

$$a \cdot y^3 + b \cdot y^2 + c \cdot y + d = 0 \tag{2.26}$$

2.4 cardano's method

Gerolamo Cardano was an Italian doctor, mathematician, philosopher and astrologer. He was recognized as the inventor of the universal joint as well as the founder of probability and the discoverer of the roots of the cubic function [6, Cardano].
Cardano's formulae of the third-order equation requires $a \neq 0$ and consequently $k_3 \neq 0$.
It is defined $y = x - \frac{b}{3a}$, replacing y with x in the third-order equation yields:

$$x^3 + \left(\frac{c}{a} - \frac{b^2}{3a^2}\right) \cdot x + \frac{d}{a} - \frac{b \cdot c}{3a^2} + \frac{2b^3}{27a^3} = 0 \tag{2.27}$$

Replacing $p = \frac{c}{a} - \frac{b^2}{3a^2}$ and $q = \frac{d}{a} - \frac{b \cdot c}{3a^2} + \frac{2b^3}{27a^3}$

$$x^3 + p \cdot x + q = 0 \tag{2.28}$$

Now Δ is defined as:

$$\Delta = \frac{q^2}{4} + \frac{p^3}{27} \tag{2.29}$$

There are three possible conditions based on the positivity of Delta, each condition yields different equations for the solutions. To proceed finding the roots it is necessary to assert the identity:

$$x = u + v \tag{2.30}$$

Powering to the third order

$$x^3 = (u + v)^3 \tag{2.31}$$

$$x^3 = u^3 + 3u^2v + 3uv^2 + v^3 \tag{2.32}$$

$$x^3 = u^3 + v^3 + 3uv \cdot (u + v) \tag{2.33}$$

$$x^3 = u^3 + v^3 + 3uv \cdot x \tag{2.34}$$

$$x^3 - 3uv \cdot x - \left(u^3 + v^3\right) = 0 \tag{2.35}$$

Based on hypothesis, the solution to this third order equation is known (the solution is $x = u + v$). So it is possible to match the coefficients of this equation with the coefficients of the reduced equation in x.

$$\begin{cases} -3uv = p \\ -\left(u^3 + v^3\right) = q \end{cases} \tag{2.36}$$

so

$$\begin{cases} uv = -\frac{p}{3} \\ u^3 + v^3 = -q \end{cases} \tag{2.37}$$

To solve for u and v, the first equation needs to be expressed in the cubic form.

$$\begin{cases} u^3v^3 = -\frac{p^3}{27} \\ u^3 + v^3 = -q \end{cases} \tag{2.38}$$

Thus, it is possible to solve for u and v as a second-order equation.

$$u = \sqrt[3]{-\frac{q}{2} + \sqrt{\Delta}} \tag{2.39}$$

$$v = \sqrt[3]{-\frac{q}{2} - \sqrt{\Delta}} \tag{2.40}$$

In the domain of complex numbers the cubic root has three solutions:

$$u_1 \, , \, u_2 \, , \, u_3$$

and

$$v_1 \, , \, v_2 \, , \, v_3$$

The total combinations of solutions are nine: u_i, v_j for $i\,,\,j\ \in\ (1,2,3)$
However, according to the first equation declared:

$$uv\ =\ -\frac{p}{3}$$

The product uv has to be a real number, so among the nine possible tuples only three respect the condition:

$$uv\ \in\ \Re$$

Specifically, only the tuples in which u_i, v_i are complex conjugate respect the above condition.

$$(u_1\,,\,v_1)\ ,\ (u_2\,,\,v_2)\ ,\ (u_3\,,\,v_3)$$

The triplet u_1, u_2, u_3 are separated by $120°$ angle in the complex plane. The same is also valid for v_1, v_2, v_3.
All the cases for Δ were analysed and the solutions extracted are shown below.
Case $\Delta > 0$

$$y_1\ =\ x_1\ -\ \frac{b}{3a}\ =-\frac{b}{3a}\ +\ u\ +\ v \tag{2.41}$$

$$y_2\ =\ x_2\ -\ \frac{b}{3a}\ =-\frac{b}{3a}\ +\ u\cdot\left(-\frac{1}{2}\ +\ i\frac{\sqrt{3}}{2}\right)\ +\ v\cdot\left(-\frac{1}{2}\ -\ i\frac{\sqrt{3}}{2}\right) \tag{2.42}$$

$$y_3\ =\ x_3\ -\ \frac{b}{3a}\ =-\frac{b}{3a}\ +\ u\cdot\left(-\frac{1}{2}\ -\ i\frac{\sqrt{3}}{2}\right)\ +\ v\cdot\left(-\frac{1}{2}\ +\ i\frac{\sqrt{3}}{2}\right) \tag{2.43}$$

Case $\Delta = 0$

$$y_1\ =\ x_1\ -\ \frac{b}{3a}\ =-\frac{b}{3a}\ -2\sqrt[3]{\frac{q}{2}} \tag{2.44}$$

$$y_2\ =\ x_2\ -\ \frac{b}{3a}\ =-\frac{b}{3a}\ +\ \sqrt[3]{\frac{q}{2}} \tag{2.45}$$

$$y_3\ =\ y_2 \tag{2.46}$$

Case $\Delta < 0$

$$\rho\cdot\,(\cos\theta\ +\ i\cdot\,\sin\theta)\ =\ -\frac{q}{2}\ +\ i\sqrt{-\Delta} \tag{2.47}$$

$$y_1\ =\ x_1\ -\ \frac{b}{3a}\ =-\frac{b}{3a}\ +2\sqrt{\frac{-p}{3}}\cdot\,\cos\frac{\theta}{3} \tag{2.48}$$

$$y_2\ =\ x_2\ -\ \frac{b}{3a}\ =-\frac{b}{3a}\ +2\sqrt{\frac{-p}{3}}\cdot\,\cos\frac{\theta+2\pi}{3} \tag{2.49}$$

$$y_3\ =\ x_3\ -\ \frac{b}{3a}\ =-\frac{b}{3a}\ +2\sqrt{\frac{-p}{3}}\cdot\,\cos\frac{\theta+4\pi}{3} \tag{2.50}$$

In the case of $\Delta\ >\ 0$:

- one solution (y_1) is real
- the other two solutions are complex conjugate (y_2, y_3)

In the case of $\Delta = 0$:

- one solution (y_1) is real
- the other two solutions are coincident (y_2, y_3)

In the case of $\Delta < 0$, so $\left(\frac{p}{3}\right)^3 < -\left(\frac{q}{2}\right)^2$:

- all the solutions (y_1, y_2, y_3) are real

The three solutions represent the zero-derivatives of the potential where two of them, y_1 and y_3 are long-term stable solutions and y_2 is the unstable solution.

3 METHODOLOGY

A new model has to be tested before being applied in the field in order to make sure its consistency and reliability.
The first order H.A.M. solution is extrapolated and it is used to generate mock data using the same parameter's values from the paper by F. Tajaddodianfar, M. R. H. Yazdi, H. N. Pishkenari [4, Non linear dynamics of MEMS/NEMS resonators], to check for repeatability of the results. The correct replication of the paper's examples proves the extrapolation of the mathematical laws to be correct. Consequently, a batch of mock data with known parameters is created in order to be fitted to check if the algorithm converge to the right solutions.
The parameters' effect on the solution and the microGauge's experimental set-up are described. Finally, real experimental data from microGauge's pressure sensor is fitted and an actuation limit potential is computed.

3.1 MOCK DATA

An industrial pressure sensor device is normally driven to have linear response thus, in the frame of Cardano's solutions it is equivalent to having $\Delta > 0$. As a consequence, an artificial batch of data with $\Delta > 0$ is created to represent the conditions similar to real laboratory experiments, then the computed data is fitted using the Python's package *lmfit* [7, LMFIT: Non-Linear Least-Square Minimization and Curve-Fitting for Python].
The sweeping variable w is the actuation frequency of the resonator and its unit is Hz. The amplitude of the resonator is derived from the conversion of a transimpedance amplifier to potential, and thus its unit is arbitrary. In the mock data generation the same convention was kept.
The parameters: k_3, k_2, λ, μ, K were chosen such that Δ has to be always greater than zero.

$$\begin{aligned} k_3 &= -0.02 \\ k_2 &= 0 \\ \lambda &= 10 \\ \mu &= 0.001 \\ K &= 0.01 \end{aligned}$$

Using the Cardano's formula 2.41 the solution was extracted only for the branch y_1 and the frequency w was swept between $9.995 \leq w \leq 10.005$.
In the code language these equivalents are made:

$$\mu = mu \tag{3.1}$$
$$\lambda = lb \tag{3.2}$$

Applying all the substitutions:

```
#The polynomial equation considered is ay^3+by^2+cy+d=0
# a is the first coefficient of the third order polynomial, f(k3)
a=9*k3**2/16
# b is the second coefficient of the third order polynomial, f(k3,lb,w)
b=3*k3*(lb**2 - w**2)/2
# c is the third coefficient of the third order polynomial, f(lb,w,mu)
c=((lb**2 - w**2)**2+(mu**2)*w**2)
# d is the last coefficient of the third order polynomial, f(K)
d= -K**2

# p is an intermidiate calculation
p= c/a - b**2/(3*a**2)
# q is an intermidiate calculation
q= d/a - b*c/(3*a**2) + 2*b**3/(27*a**3)

# Delta controls the number of real solution,
#thus the stability of the resonator
delta = q**2/4 + p**3/27
#initialization
u = np.zeros(len(delta))
v = np.zeros(len(delta))

y1 = np.zeros(len(w))
```

The real solution of the third order equation was computed.

```
#Performs a loop to assign an amplitude for each frequency (w) value
for i in range(0, len(w)):
        #Case of Delta>0
        if delta[i] > 0:
                #Those nested 'if' gives to u only
                #the real solution of cubic root
                if -q[i]/2+mp.sqrt(delta[i]) > 0:
                        u[i]= mp.cbrt(-q[i]/2+mp.sqrt(delta[i]))
                elif -q[i]/2+mp.sqrt(delta[i]) < 0:
```

```
                    u[i]= -mp.cbrt(np.abs(-q[i]/2+mp.sqrt(delta[i])))
                else:
                    u[i]= 0
                #Nested 'if' for v, it gives only
                #the real solution of cubic root
                if -q[i]/2-mp.sqrt(delta[i]) > 0:
                    v[i]= mp.cbrt(-q[i]/2-mp.sqrt(delta[i]))
                elif -q[i]/2-mp.sqrt(delta[i]) < 0:
                    v[i]= -mp.cbrt(np.abs(-q[i]/2-mp.sqrt(delta[i])))
                else:
                    v[i]= 0
                # real amplitude solution
                y1[i] = -b[i]/(3*a) + u[i] + v[i]
        else:
                # check is there are any negative values
                raise ValueError('delta has to be greater than 0.')
```

Previously it was declared $y = z^2$, so the conversion of y gives the solution of H.A.M.

$$z = \sqrt{y}$$

The following figure 3.1 represents the case k_3 close to zero and $\Delta > 0$ everywhere.

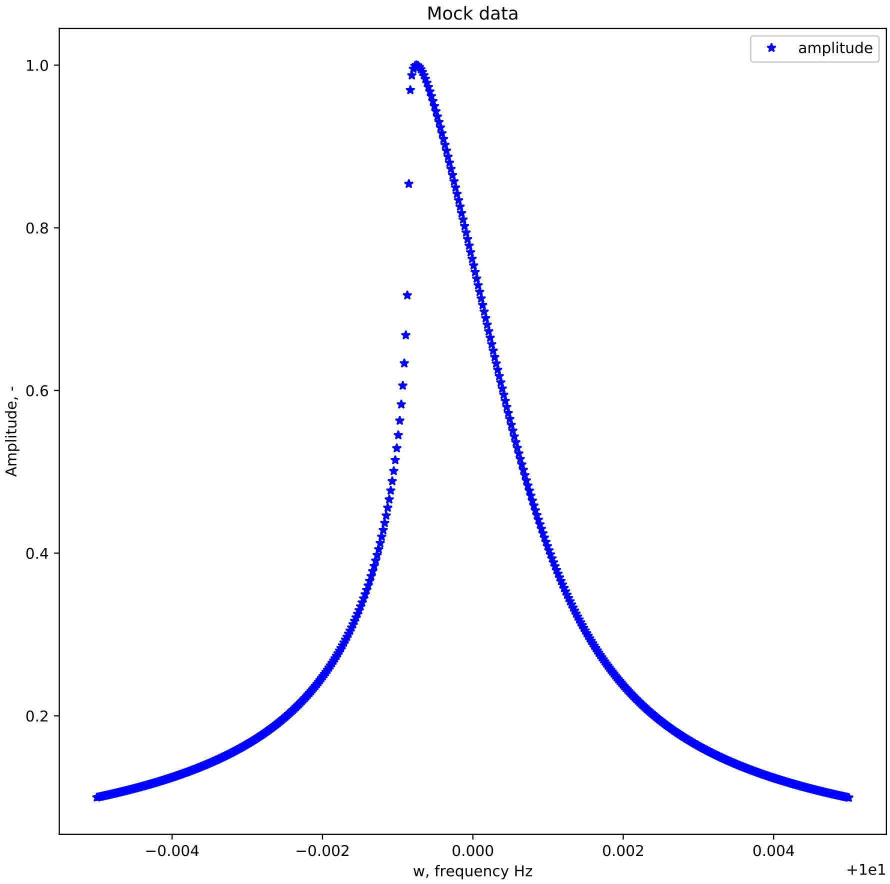

Figure 3.1: Plot of the mock data with the coefficients $k_3 = -0.02$, $k_2 = 0$, $\lambda = 10$, $\mu = 0.001$, $K = 0.01$. This image was generated through Python script

3.2 PARAMETERS ANALYSIS

The positivity of Δ is very important to understand the phenomenological behaviour of the resonator as well as its relationship with the physical parameters. First, the formula is expanded until the Duffing's parameters become visible.

$$\Delta = \frac{\left(3ac - b^2\right)^2}{36a^4} + \frac{\left(27a^2 d - 9abc + 2b^3\right)^3}{27^4 a^9} \tag{3.3}$$

$$\Delta = \frac{1}{9a^4} \cdot \left[\frac{9a^2c^2 + b^4 - 6ab^2c}{4} + \frac{\left(27a^2 d - 9abc + 2b^3\right)^3}{3^{10} a^5} \right] \tag{3.4}$$

it can be re-written as:

$$\Delta = \frac{27a^2d^2 - 18abcd + 4ac^3 + 4b^3d - b^2c^2}{108a^4} \tag{3.5}$$

With k_3, lb, mu, K parameters:

$$\Delta = \frac{64}{81k_3^4} \cdot \left[K^2 + \frac{8}{81}\left(lb^2 - w^2\right)^2 + 9w^2mu^2\right]^2 + \frac{4096}{729k_3^6} \cdot \left[mu^2w^2 - \frac{\left(lb^2 - w^2\right)^2}{3}\right]^3 \tag{3.6}$$

The Jacobian of Δ is composed of:

$$\frac{\partial \Delta}{\partial k_3} = -\frac{1}{k_3} \cdot \left(q^2 + \frac{2p^3}{9}\right) \tag{3.7}$$

$$\frac{\partial \Delta}{\partial K} = -\frac{16qK}{9k_3^2} \tag{3.8}$$

$$\frac{\partial \Delta}{\partial mu} = \frac{32 \cdot mu \cdot w^2}{81k_3^2} \cdot \left(-4q \cdot \left(lb^2 - w^2\right) + p^2\right) \tag{3.9}$$

$$\frac{\partial \Delta}{\partial lb} = \frac{64lb}{81k_3^2} \cdot \left[-2q \cdot \left(\frac{(lb^2 - w^2)^2}{3} + mu^2w^2\right) + \frac{p^2 \cdot \left(w^2 - lb^2\right)}{3}\right] \tag{3.10}$$

The value of Δ is totally positive when k_3 is close to zero. For increasing values of k_3 it would be divided into three parts, a range of frequencies to the left where $\Delta > 0$, a center range where $\Delta < 0$ and the remaining part where $\Delta > 0$.

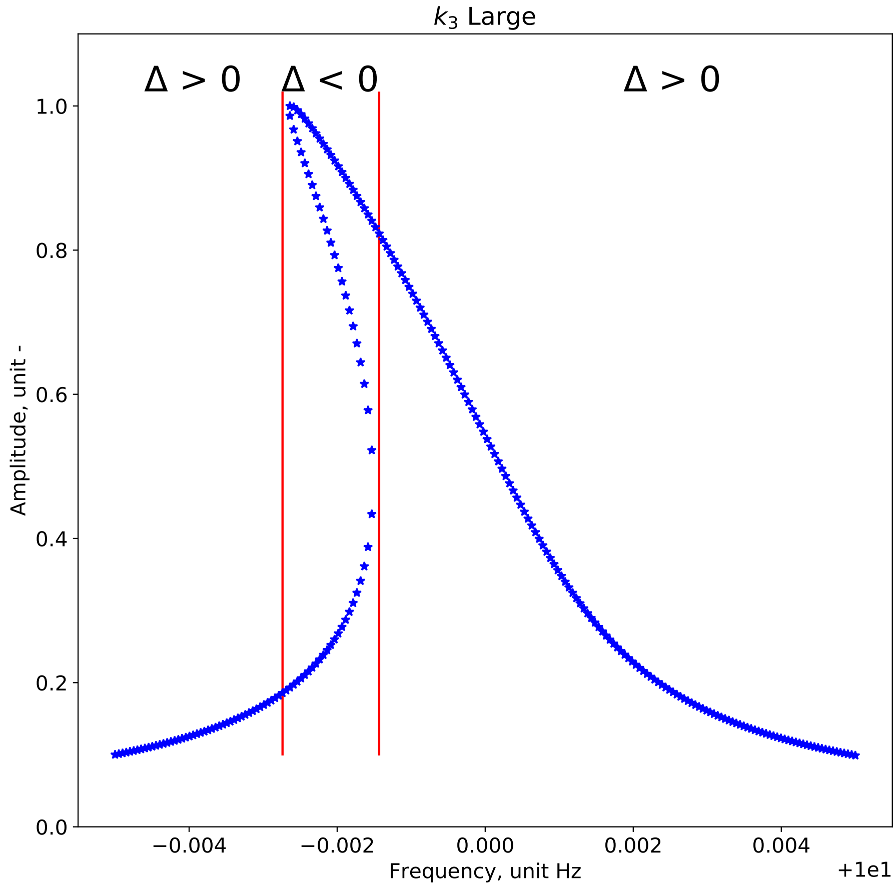

Figure 3.2: According to the skewness of the data, the plot can be divided into three parts, the parts that have only one real solution, in which $\Delta > 0$, and the part with three real solutions, in which $\Delta < 0$. This image was generated through Python script

In the frame of H.A.M., the k_3 controls only the curve's skew, hence the non linearity of the function.

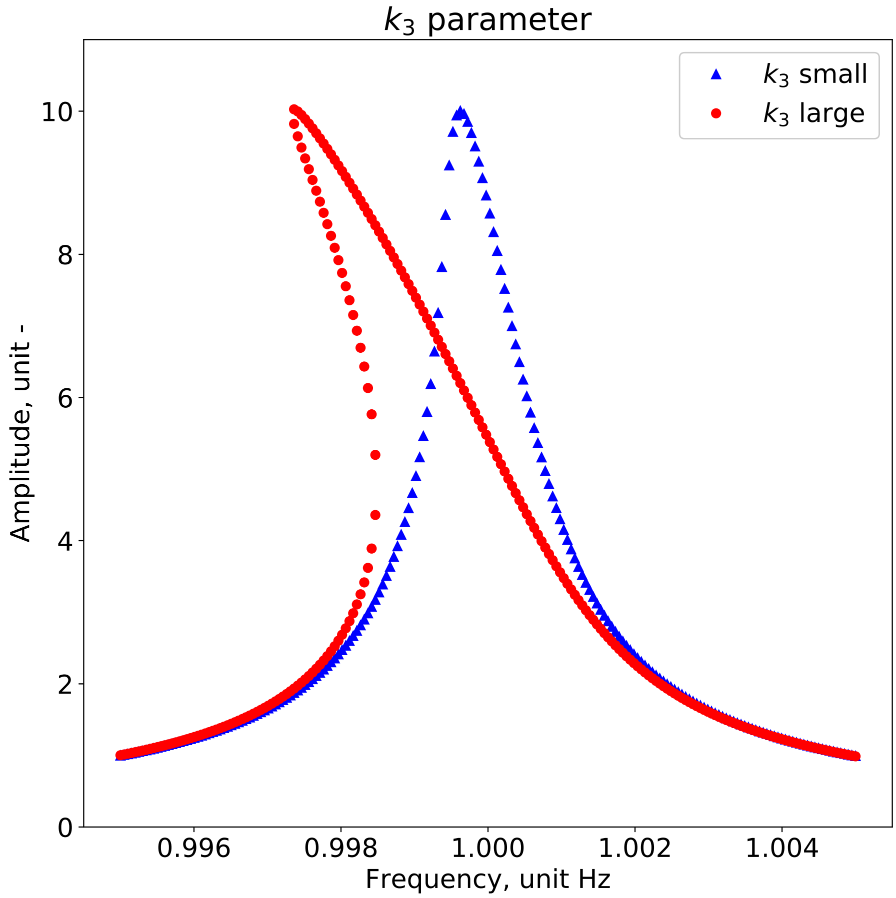

Figure 3.3: The parameter k_3 is directly proportional to the skewness of the plot, it would lean towards the left in the case of softening, and towards the right in the case of hardening. This image was generated through Python script

The viscosity parameter μ would enlarge the curve and decrease the peak's value, if too large it can resolve the curve to Lorentzian-like:

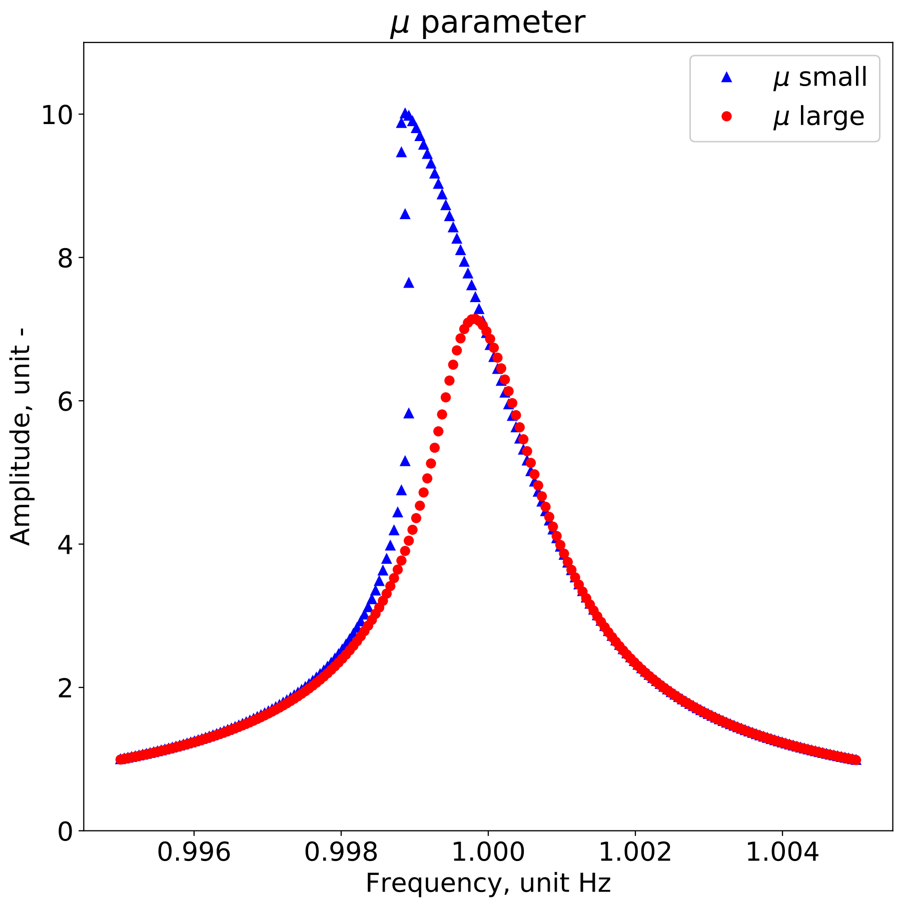

Figure 3.4: The parameter μ is inversely proportional to the quality factor. This image was generated through Python script

The K parameter is proportional to the force applied to the resonator thus, $K \propto (V_{AC} + V_{DC})^2$. It controls the amplitude and the curve's skew.

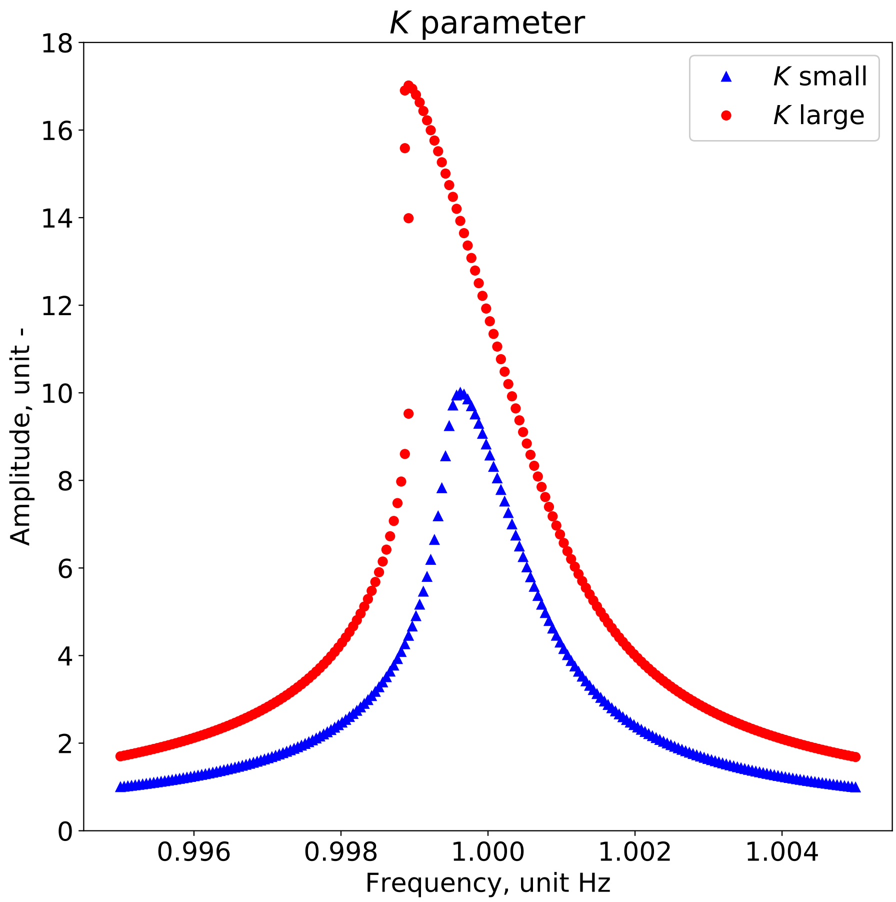

Figure 3.5: The parameter K is directly proportional to the square of the actuation potential, it influences the peak's amplitude and the non linearity. This image was generated through Python script

3.3 FITTING

In this section, the procedure to fit the generated data and the outcome quality of this algorithm are presented. To check for the robustness, first the mock data is fitted and the parameters are compared with the initial coefficients, then the procedure is applied to the experimental data.

3.3.1 Fitting mock data

The fitting procedure uses the Python package **lmfit** [8, LMFIT: Non-Linear Least-Square Minimization and Curve-Fitting for Python], which performs *least-squares* fitting and calculates the residuals.
The residuals are the differences in amplitude values between the points calculated through the

estimated parameters and the given amplitude points. The residuals are minimized in the sum least-square mean varying the three parameters in an iterative loop.

$$residuals = \sum_i^N (z_{i,estimated} - z_i)^2 \tag{3.11}$$

In the case of $\Delta > 0$ only one solution is real, thus the fitting is constrained to one point. In the case of $\Delta < 0$, instead, there are three real solutions, and thus the program will select the solution with the minor module difference with respect to the experimental data point.

$$i = \min_{index}(||z_n - y_1||, ||z_n - y_2||, ||z_n - y_3||) \tag{3.12}$$

$$z_{estimated} = \sqrt{y_i} \tag{3.13}$$

The centre of the frequency axes is the initial condition for the resonant frequency (λ). It is an accurate approximation of the real resonance frequency.
The correct parameters, those used to generate the data are:

- $k_3 = -3 \cdot 10^{-5}$
- $\lambda = 1$
- $\mu = 10^{-3}$
- $K = 10^{-2}$

Their boundaries are defined to have a reasonable domain near the estimated value.

$$\lambda_{max} = max(w) \quad \text{upper boundary of resonance frequency} \tag{3.14}$$
$$\lambda_{min} = min(w) \quad \text{lower boundary of resonance frequency} \tag{3.15}$$
$$k_{3,max} = -10^{-8} \quad \text{upper boundary of non linear term} \tag{3.16}$$
$$k_{3,min} = -1 \quad \text{lower boundary of non linear term} \tag{3.17}$$
$$\mu_{max} = 1 \quad \text{upper boundary of viscosity} \tag{3.18}$$
$$\mu_{min} = 10^{-4} \quad \text{lower boundary of viscosity} \tag{3.19}$$
$$K_{max} = +\infty \quad \text{upper boundary of actuation parameter} \tag{3.20}$$
$$K_{min} = 0 \quad \text{lower boundary of actuation parameter} \tag{3.21}$$

To study the effect of different initial conditions to the fitting function, a three nested sweeps was performed in loop.

1. $k_{3,estimated} = \textit{First value of first parameter}$
   $\mu_{estimated} = \textit{value of second parameter}$
   $K_{estimated} = \textit{Sweeping value}$
   ...
   ...

Through this method all possible estimated values are used in the fitting function.

$$k_{3,estimated} = [-10^{-7}, -10^{-6}, -10^{-5}, -10^{-4}, -10^{-3}] \tag{3.22}$$

$$\mu_{estimated} = [10^{-4}, 10^{-3}, 10^{-2}] \tag{3.23}$$

$$K_{estimated} = [10^{-4}, 10^{-3}, 10^{-2}, 10^{-1}, 1] \tag{3.24}$$

The function that calculates the $z_{estimated}$ using $k_{3,estimated}$, $\mu_{estimated}$, $K_{estimated}$ is defined as:

```
#This function calculates the amplitude for given parameters (k3 ,mu, lb ,K)
#the fitting program would first estimate the
#paramters' values close to the supposed solution
#then it will vary them according to the minimum residuals value obtained
def sol(w, k3, lb, mu, K):
        #first polynomial coefficient
        a=9*k3**2/16
        #second polynomial coefficient
        b=3*k3*(lb**2 - w**2)/2
        #third polynomial coefficient
        c=((lb**2 - w**2)**2+(mu**2)*w**2)
        #last polynomial coefficient
        d= -K**2
        # intermidiate computations
        p= c/a - b**2/(3*a**2)
        q= d/a - b*c/(3*a**2) + 2*b**3/(27*a**3)
        # Delta controls the number of real solutions
        delta = q**2/4 + p**3/27
        #initialization
        u = np.zeros(len(w))
        v = np.zeros(len(w))
        z= np.zeros(len(w))
        y1= np.zeros(len(w))
        y2= np.zeros(len(w))
        y3= np.zeros(len(w))
        # loop to assign an amplitude to each frequency's value (w)
        for i in range(0, len(w)):
                # Condition for delta>0, one real solution
                # and two complex solutions
                if delta[i] > 0:
                        #nested 'if' for u, it gives only the real solution
                        # of cubic root
```

```
    if -q[i]/2+mp.sqrt(delta[i]) > 0:
        u[i]= mp.cbrt(-q[i]/2+mp.sqrt(delta[i]))
    elif -q[i]/2+mp.sqrt(delta[i]) < 0:
        u[i]= -mp.cbrt(np.abs(-q[i]/2+mp.sqrt(delta[i])))
    else:
        u[i]= 0
    #nested 'if' for v, it gives only the real solution
    # of cubic root
    if -q[i]/2-mp.sqrt(delta[i]) > 0:
        v[i]= mp.cbrt(-q[i]/2-mp.sqrt(delta[i]))
    elif -q[i]/2-mp.sqrt(delta[i]) < 0:
        v[i]= -mp.cbrt(mp.fabs(-q[i]/2-mp.sqrt(delta[i])))
    else:
        v[i]= 0
    if -b[i]/(3*a) + u[i] + v[i] > 0:
        z[i] = mp.sqrt(-b[i]/(3*a) + u[i] + v[i])
    else:
        z[i] = 0
# Condition for delta==0, one real solution
# and two coincident solutions
elif delta[i] == 0:
    if q[i] > 0:
        y1[i] = mp.sqrt(-b[i]/(3*a) -2*(q[i]/2)**(1./3.))
        y2[i] = mp.sqrt(-b[i]/(3*a) + (q[i]/2)**(1./3.))
    elif q[i] < 0:
        y1[i] = mp.sqrt(-b[i]/(3*a) +
                        2*(mp.cbrt(ny.abs(q[i]/2))))
        y2[i] = mp.sqrt(-b[i]/(3*a) +
                        -mp.cbrt(np.abs(q[i]/2)))
    else:
        y1[i] = mp.sqrt(-b[i]/(3*a))
        y2[i] = y1[i]
    y3[i] = y2[i]
    if np.abs(amp[i]-y1[i]) < np.abs(amp[i]-y3[i]):
        z[i] = y1[i]
    else:
        z[i] = y2[i]
# Condition delta<0, three real solutions, z has the point
# closer to the amplitude data
else:
    angle = mp.phase( -q[i]/2 - mp.sqrt(delta[i]))
```

```
            y1[i] = mp.sqrt(-b[i]/(3*a) +
                    2*mp.sqrt(-p[i]/3)*mp.cos(angle/3))
            y2[i] = mp.sqrt(-b[i]/(3*a) +
                    2*mp.sqrt(-p[i]/3)*mp.cos(angle/3+2*(mp.pi)/3))
            y3[i] = mp.sqrt(-b[i]/(3*a) +
                    2*mp.sqrt(-p[i]/3)*mp.cos(angle/3+4*(mp.pi)/3))
            # Choose the y value with module difference closer
            # to the input amplitude
            if np.abs(amp[i]-y1[i]) <
                    min(np.abs(amp[i]-y3[i]), np.abs(amp[i]-y2[i])):
                    z[i] = y1[i]
            elif np.abs(amp[i]-y2[i]) < np.abs(amp[i]-y3[i]):
                    z[i] = y2[i]
            else:
                    z[i] = y3[i]
    return z
```

3.3.2 Fitting results

The package **lmfit** provides useful tools to check the properties of the fitting. Lmfit calculates the *Goodness-of-fit* statistics and provides different methods to calculate the residuals. The *Goodness-of-fit* statistic is described in table 3.1.
In figure 3.6 there is an example of good fitting with some injected noise into the data, the noise was generated through a random digital value.

Table 3.1: Table of the *Goodness-of-fit* provided by the package *lmfit*

Attributes	Description
nfev	number of function evaluations
nvarys	number of variables in the fit N_{varys}
ndata	number of data points: N
nfree	degrees of freedom in the fit: $N - Nvarys$
residual	residual array, $[Resid_i]$
chisqr	chi-square: $\chi^2 = \sum_i^N [Resid_i]^2$
redchi	reduced chi-square: $\chi_\nu^2 = \frac{\chi^2}{N - N_{varys}}$
aic	Akaike information criterion statistic
bic	Bayesian information criterion statistic
var-names	ordered list of variables parameters names
covar	covariance matrix
init-vals	list of initial values for variable parameters

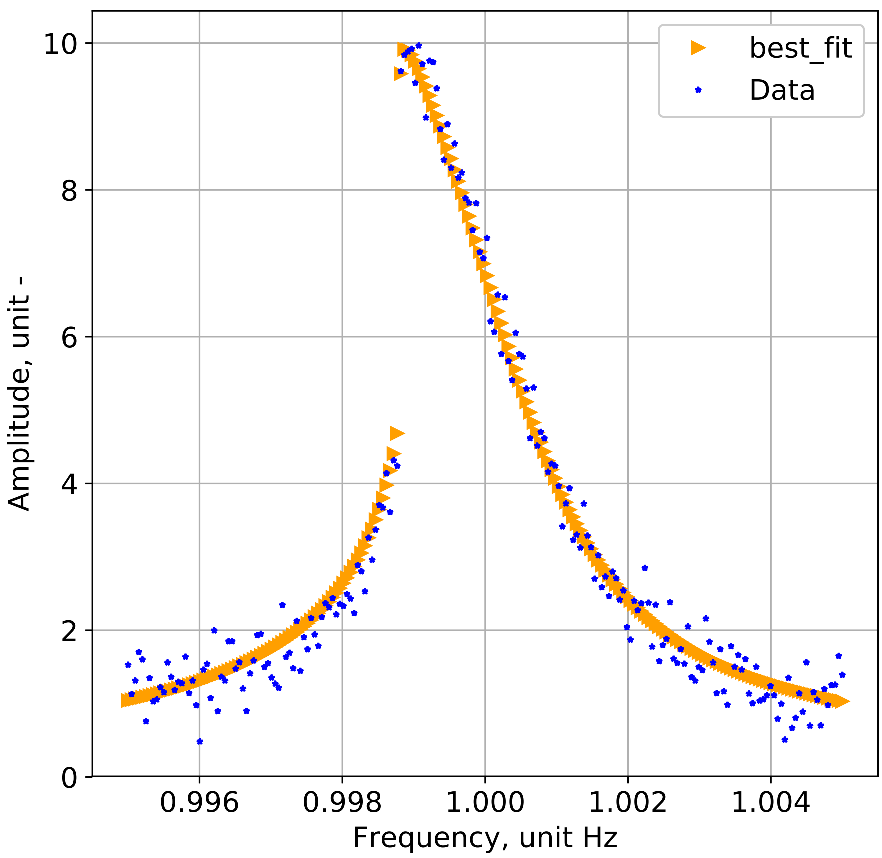

Figure 3.6: Example of mock data fitted correctly, the extracted parameters can be visible on a separate report. This image was generated through Python script

The resulting report is in the following.

```
[[Model]]
        Model(FirstOrderHAM)
[[Fit Statistics]]
        # fitting method   = leastsq
        # function evals   = 143
        # data points      = 200
        # variables        = 3
        chi-square         = 19.8613523
        reduced chi-square = 0.10081905
        Akaike info crit   = -455.908324
        Bayesian info crit = -446.013372
[[Variables]]
        k3:  -3.0175e-05 +/- 1.2603e-09 (0.00%) (init = -1e-05)
        lb:  1 (fixed)
        mu:  0.00105292 +/- 2.2752e-05 (2.16%) (init = 0.001)
        K:   0.01043445 +/- 1.2235e-04 (1.17%) (init = 0.01)
[[Correlations]] (unreported correlations are < 0.100)
        C(k3, mu) = -0.915
        C(mu, K)  =  0.731
        C(k3, K)  = -0.394
```

In case the fitting did not succeed the function would not be able to calculate the uncertainties on the parameters and coefficients' values will not be meaningful.

```
[[Model]]
        Model(FirstOrderHAM)
[[Fit Statistics]]
        # fitting method   = leastsq
        # function evals   = 10
        # data points      = 200
        # variables        = 3
        chi-square         = 2247.77408
        reduced chi-square = 11.4100207
        Akaike info crit   = 489.875669
        Bayesian info crit = 499.770621
[[Variables]]
        k3:  -1.0000e-06 +/- 1.6037e-06 (160.37%) (init = -1e-06)
        lb:  1 (fixed)
        mu:  1.0000e-04 +/- 6.0197e-14 (0.00%) (init = 0.0001)
        K:   1.0000e-03 +/- 2.0719e-04 (20.72%) (init = 0.001)
[[Correlations]] (unreported correlations are < 0.100)
```

```
C(mu, K) = 0.196
```

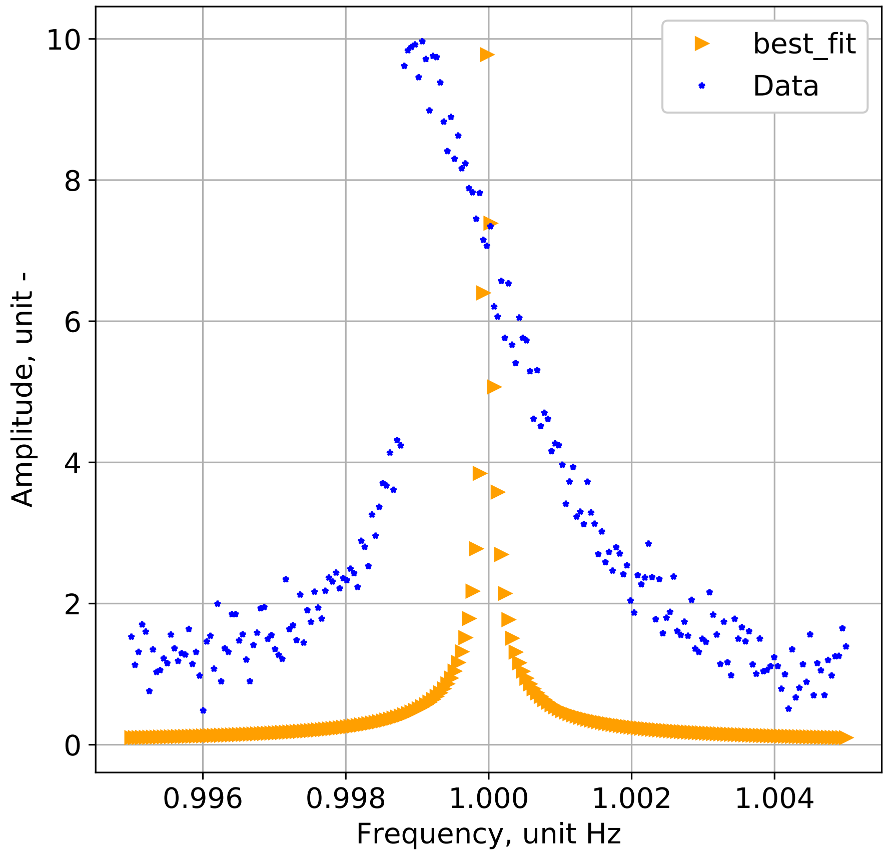

Figure 3.7: Example of fitting curve that does not match with data. This image was generated through Python script

In conclusion, three different graphs were produced where each of them had one $\mu_{estimated}$ value fixed. Following that, k_3 value was extracted, plotted and confronted with the real k_3 (the red horizontal line). In figure 3.8 every point represents a fitted parameter k_3.

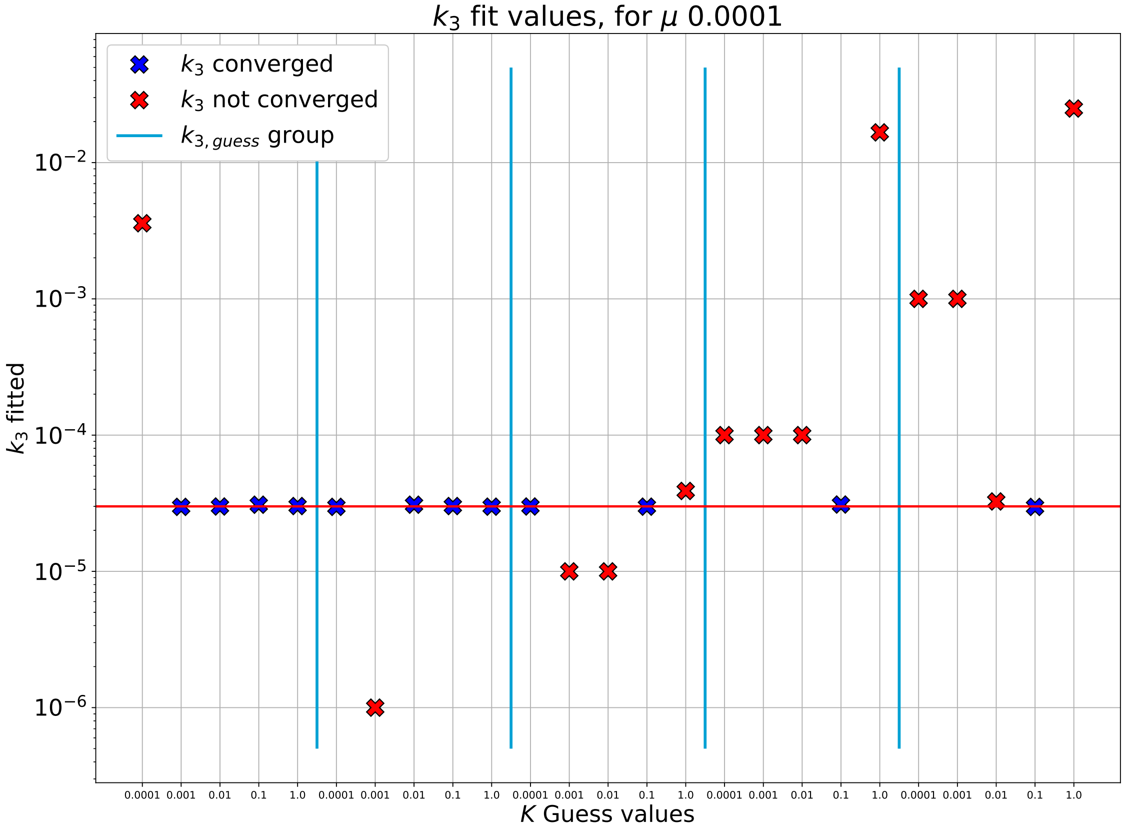

Figure 3.8: In this graph the $\mu_{estimated}$ is 0.0001, on the x-axis different values of $K_{estimated}$ swept are shown. $K_{estimated}$ is swept with the values $[10^{-4}, 10^{-3}, 10^{-2}, 10^{-1}, 1]$, while $k_{3,estimated}$ between $[-10^{-7}, -10^{-6}, -10^{-5}, -10^{-4}, -10^{-3}]$. Every 5 values of $K_{estimated}$ represent a fitting with a certain $k_{3,estimated}$. Since this is a semi-logarithmic plot, it was taken the module of k_3 values. This image was generated through Python script

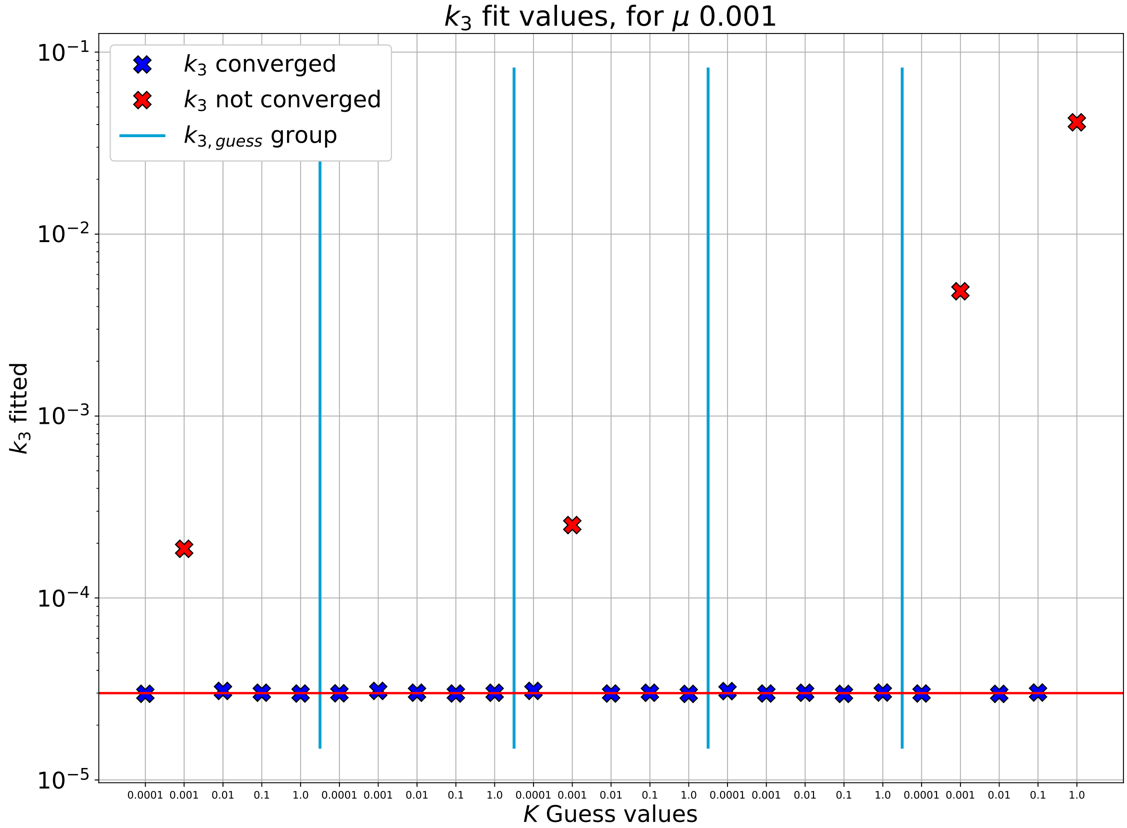

Figure 3.9: In this graph the $\mu_{estimated}$ is 0.001, on the x-axis different values of $K_{estimated}$ swept are shown. $K_{estimated}$ is swept with the values $[10^{-4}, 10^{-3}, 10^{-2}, 10^{-1}, 1]$, while $k_{3,estimated}$ between $[-10^{-7}, -10^{-6}, -10^{-5}, -10^{-4}, -10^{-3}]$. Every 5 values of $K_{estimated}$ represent a fitting with a certain $k_{3,estimated}$. Since this is a semi-logarithmic plot, it was taken the module of k_3 values. This image was generated through Python script

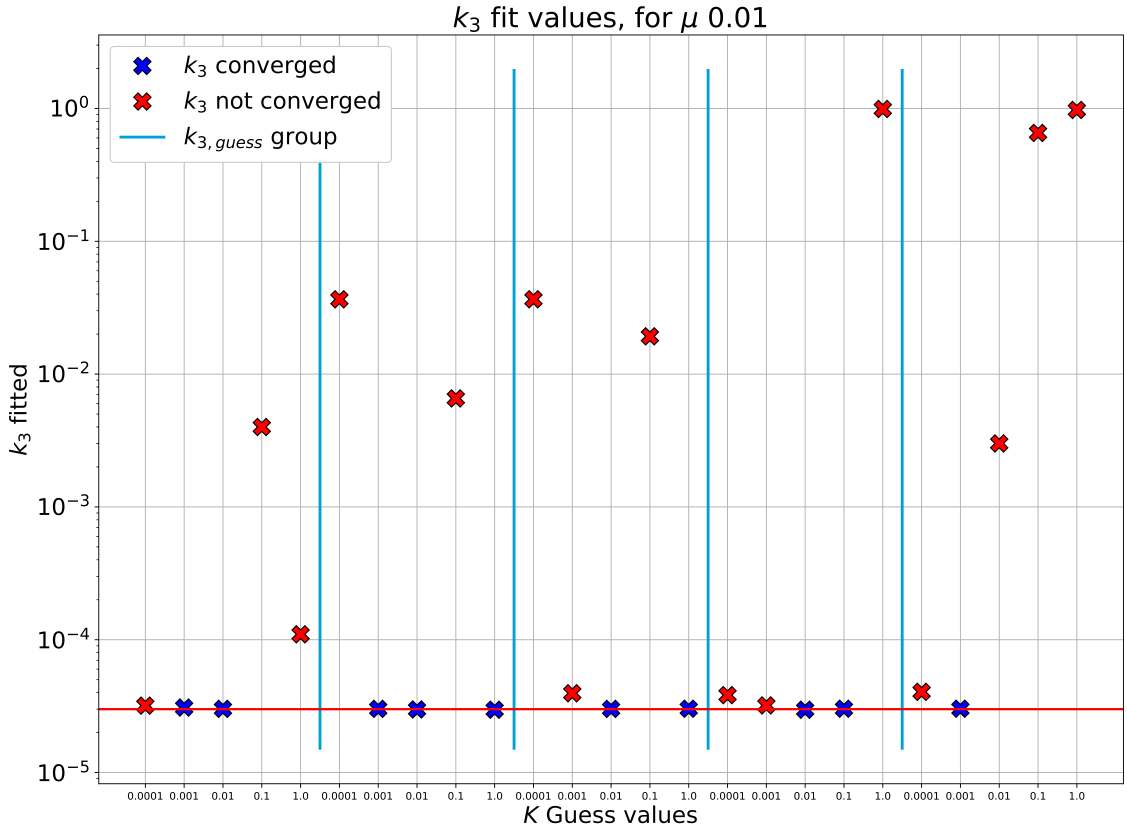

Figure 3.10: In this graph the $\mu_{estimated}$ is 0.01, on the x-axis different values of $K_{estimated}$ swept are shown. $K_{estimated}$ is swept with the values $[10^{-4}, 10^{-3}, 10^{-2}, 10^{-1}, 1]$, while $k_{3,estimated}$ between $[-10^{-7}, -10^{-6}, -10^{-5}, -10^{-4}, -10^{-3}]$. Every 5 values of $K_{estimated}$ represent a fitting with a certain $k_{3,estimated}$. Since this is a semi-logarithmic plot, it was taken the module of k_3 values. This image was generated through Python script

The fitting function was tested with estimate values for k_3 ranging 5 different orders of magnitudes, μ estimate ranging 3 diverse orders of magnitude and K, 5 orders of magnitude.
To resume, the correct parameters are:

- $k_3 = -3 \cdot 10^{-5}$
- $\lambda = 1$
- $\mu = 10^{-3}$
- $K = 10^{-2}$

The estimate values used to fit the data are:

$$k_{3,estimated} = [-10^{-7}, -10^{-6}, -10^{-5}, -10^{-4}, -10^{-3}] \tag{3.25}$$

$$\mu_{estimated} = [10^{-4}, 10^{-3}, 10^{-2}] \tag{3.26}$$

$$K_{estimated} = [10^{-4}, 10^{-3}, 10^{-2}, 10^{-1}, 1] \tag{3.27}$$

The values of failed fits were discarded. The criteria of passing/failing fit is:

$$-3.1 \cdot 10^{-5} \leq k_3 \leq -2.9 \cdot 10^{-5}$$

- For $\mu_{estimated} = 10^{-4}$ => 13 fittings were rejected among 25
- For $\mu_{estimated} = 10^{-3}$ => 4 fittings were rejected among 25
- For $\mu_{estimated} = 10^{-2}$ => 15 fittings were rejected among 25

Taking one parameter fixed, the average and standard deviation of k_3 were computed.

- For $\mu_{estimated} = 10^{-4}$ => $k_{3,mean} = -3.015 \cdot 10^{-5}$, $k_{3,\sigma} = 1.68 \cdot 10^{-6}$
- For $\mu_{estimated} = 10^{-3}$ => $k_{3,mean} = -3.012 \cdot 10^{-5}$, $k_{3,\sigma} = 2.20 \cdot 10^{-6}$
- For $\mu_{estimated} = 10^{-2}$ => $k_{3,mean} = -3.013 \cdot 10^{-5}$, $k_{3,\sigma} = 1.62 \cdot 10^{-6}$

The outcome proves that the fitting function is highly sensitive to the initial value of $\mu_{estimated}$. If $\mu_{estimated}$ is close to the the exact solution, the probability that the fitted k_3 intersects the solution with an accuracy of ± 0.1 is 84.0%.
In the case where $\mu_{estimated}$ is one order of magnitude away from the exact solution, the probability that the fitted k_3 intersects the solution with an accuracy of ± 0.1 is 40.0%. Thus, in the experimental data fitting a procedure to compute the value of μ was implemented.

3.4 FITTING EXPERIMENTAL DATA

The fitting procedure was proved accurate for artificially generated data. The next step consists of parameters extraction from real experimental data.
This section describes the laboratory set-up of microGauge, the specific sensors used for experiments and their outcome.

3.4.1 Set-up

The experimental set-up consists of a vacuum chamber connected to two pumps, a nitrogen gas bottle, an automatic flow controller, pressure and temperature sensors, butterfly valve, flow pipes to the gas tank and microGauge electronics boards. The first stage pump is a liquid-oil pump able to lower the pressure in the chamber up to $1 \cdot 10^{-2}$ mbar.
The second stage pump is a turbo molecular pump, able to shift the chamber pressure from $1 \cdot 10^{-2}$ mbar to $1 \cdot 10^{-7}$ mbar. It is connected to the chamber through the butterfly valve.
The vacuum chamber is connected to a nitrogen tank with an automated flow-control system, that is able to regulate the inlet through a fine screw. In figure 3.11 a schematic of the apparatus is presented:

- MicroGauge sensors
- several third-party sensors for calibration
- two resistive gauge temperature sensors Pt1000

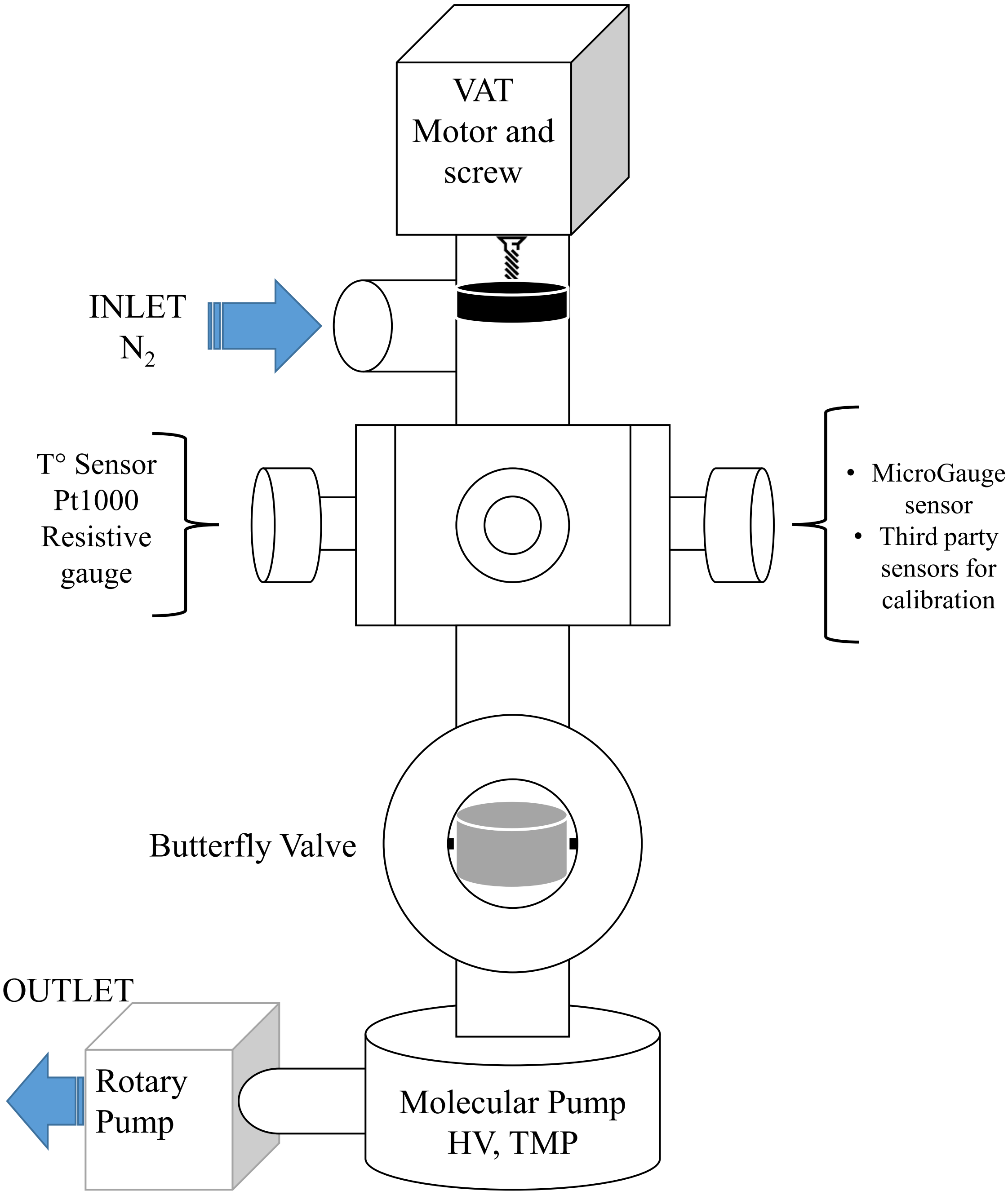

Figure 3.11: Schematic of the experimental apparatus of microGauge with an automatic flow controller at the top that moves a fine screw to open/close the inlet. Several sensors and temperature resistive gauges are attached to the vacuum chamber to cover a large range of pressures and temperatures. At the bottom of the vacuum chamber the butterfly valve provides an intermediate connection with the turbo molecular pump, which is connected with the first stage rotary pump. This image was generated through Microsoft Office PowerPoint

The transduction method consists of a capacitance read-out. In figure 3.12 the schematic is shown.

1. The top electrode is attached to the sensor's moving part, it actuates the device by applying an alternating potential
2. The sensor can be approximated to a parallel place capacitor
3. The microGauge's electronics board can be approximated to a black box, it gives the read-out signal

The signal analysis was made through a custom electronic board exclusive of microGauge.

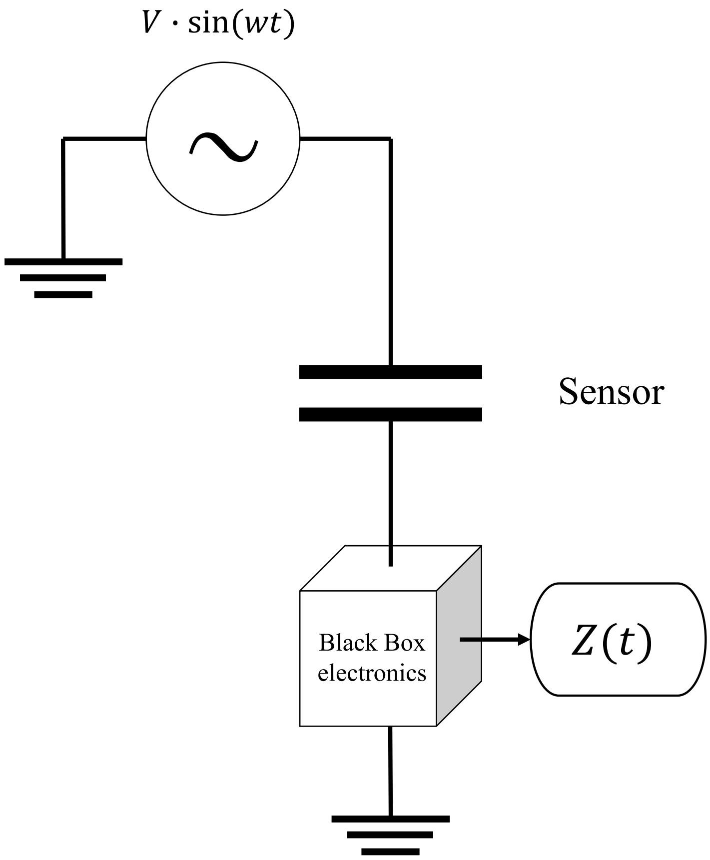

Figure 3.12: The sensor can be considered as a suspended mass with four electrodes that provide actuation as well as sensitivity. In the schematic $V_r \sin(w_r t)$ is equal to V_{outB}. This image was generated through Microsoft Office PowerPoint

3.4.2 Fitting of the experimental data

Before applying the algorithm to the experimental data, multiple data sets were fitted with Lorentzian curve, in order to extract the average and standard deviation of the viscosity parameter.
It is supposed that the viscosity remains constant during all the experiments and equal to the F.W.H.M. (full width at half maximum) of the curves. In figure 3.13 it is shown one plot as well as the outcome report.

```
[[Model]]
    Model(lorentzian, prefix='Loren_')
[[Fit Statistics]]
    # fitting method   = leastsq
    # function evals   = 13
    # data points      = 25
    # variables        = 3
    chi-square         = 107.248387
    reduced chi-square = 4.87492670
    Akaike info crit   = 42.4067924
    Bayesian info crit = 46.0634199
[[Variables]]
    Loren_sigma:      0.03832561 +/- 2.3828e-04 (0.62%) (init = 0.0337035)
    Loren_center:     1551.24195 +/- 1.4307e-04 (0.00%) (init = 1551.245)
    Loren_amplitude:  42.1832643 +/- 0.21736442 (0.52%) (init = 44.3161)
    Loren_fwhm:       0.07665123 +/- 4.7656e-04 (0.62%)
    Loren_height:     350.349262 +/- 0.91692307 (0.26%)
[[Correlations]] (unreported correlations are < 0.100)
    C(Loren_sigma, Loren_amplitude)  =  0.911
    C(Loren_center, Loren_amplitude) = -0.146
```

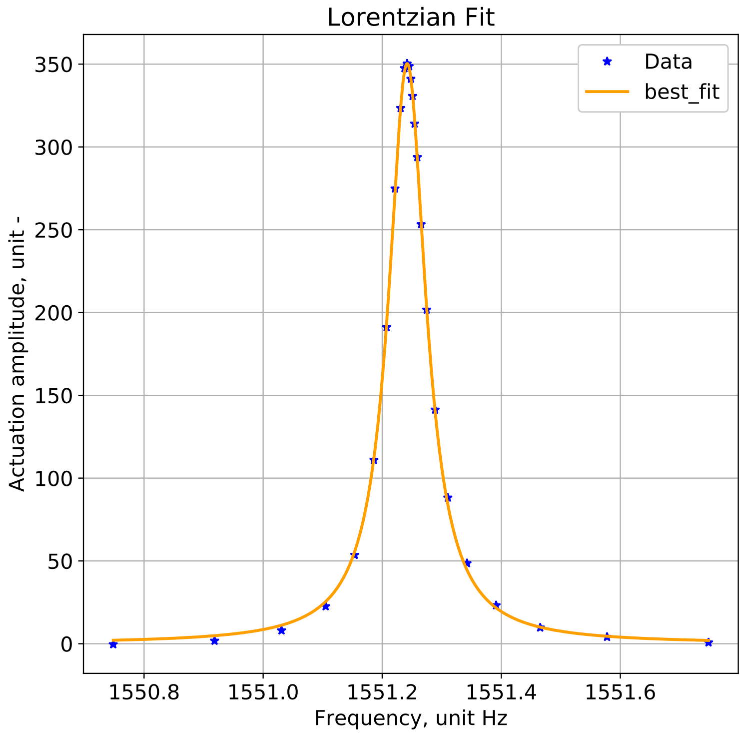

Figure 3.13: Lorentzian fitting of the sensor's data. This intermediate step is necessary to extract μ. This image was generated through Python script

Thus, the μ parameter is 0.077 ± 0.0020.
In the section 3.1, the fitting algorithm was explained, now it will be applied to an experimental set of data.
The initial condition of the parameter μ was extracted from the Lorentzian curve. The boundaries of the parameters are:

$$\lambda_{max} = max(w) \qquad \text{upper boundary of resonance frequency} \tag{3.28}$$

$$\lambda_{min} = min(w) \qquad \text{lower boundary of resonance frequency} \tag{3.29}$$

$$k_{3,max} = -10^{-8} \qquad \text{upper boundary of non linear term} \tag{3.30}$$

$$k_{3,min} = -1 \qquad \text{lower boundary of non linear term} \tag{3.31}$$

$$\mu_{max} = 1 \qquad \text{upper boundary of viscosity} \tag{3.32}$$

$$\mu_{min} = 10^{-4} \qquad \text{lower boundary of viscosity} \tag{3.33}$$

$$K_{max} = +\infty \qquad \text{upper boundary of actuation parameter} \tag{3.34}$$

$$K_{min} = 0 \qquad \text{lower boundary of actuation parameter} \tag{3.35}$$

The fit with alternating potential $V_{outB} = 0.13\,V$ is reported, figure 3.14.

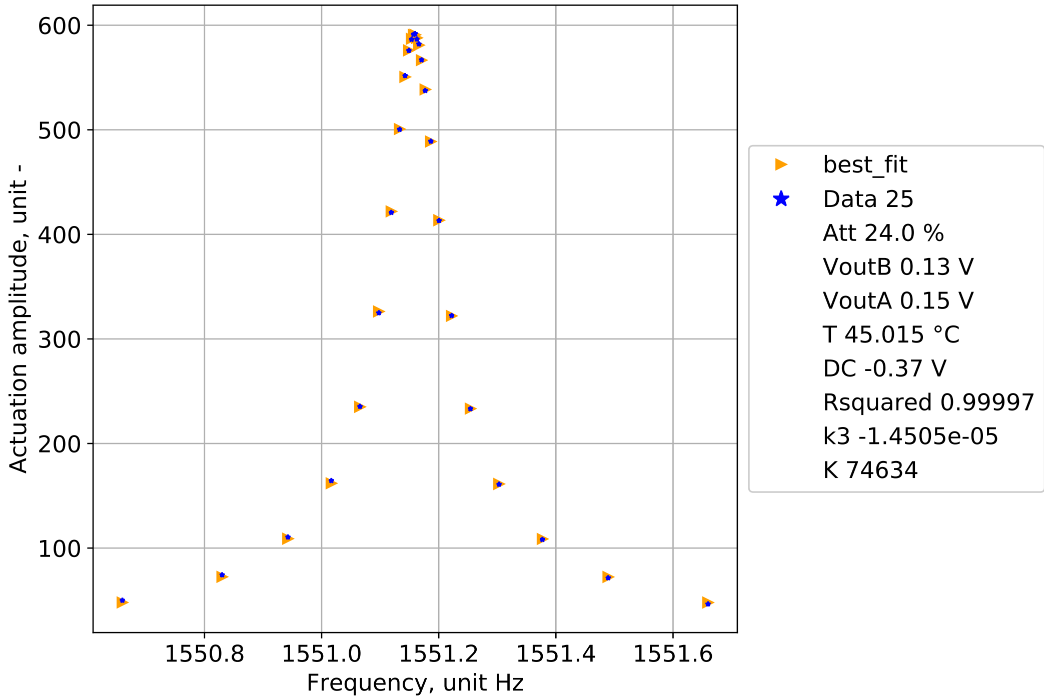

Figure 3.14: H.A.M. fitting of the experimental data. With an intermediate actuation potential the fitting has an $R^2 = 0.9999$, the extracted parameters are reported. This image was generated through Python script

```
[[Model]]
    Model(FirstOrderHAM)
[[Fit Statistics]]
    # fitting method   = leastsq
    # function evals   = 46
    # data points      = 25
    # variables        = 4
    chi-square         = 29.9154983
    reduced chi-square = 1.42454754
    Akaike info crit   = 12.4875214
    Bayesian info crit = 17.3630247
[[Variables]]
    k3:  -1.4505e-05 +/- 3.9507e-06 (27.24%) (init = -2.5e-05)
    lb:   1551.15953 +/- 2.3026e-04 (0.00%) (init = 1551.242)
    mu:   0.08138200 +/- 1.9088e-04 (0.23%) (init = 0.07753837)
    K:    74634.3225 +/- 148.296779 (0.20%) (init = 130000)
[[Correlations]] (unreported correlations are < 0.100)
    C(mu, K)  =  0.956
```

C(k3, lb) = −0.941

The figure 3.15 shows the extraction of k_3 parameter from the fitting of multiples experiments with $R^2 > 0.99$ and $k_{3,std}$ less than 25% of k_3 value:

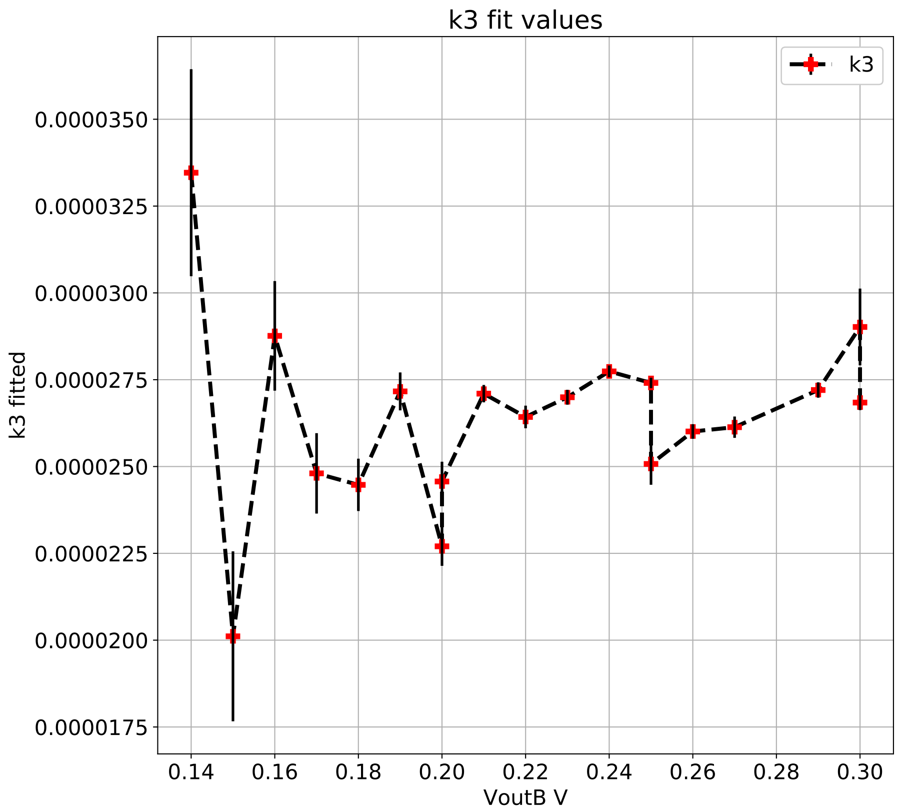

Figure 3.15: Summary of k_3 extraction with H.A.M. fitting. The red crosses represent the extracted value while the vertical black lines refer to the standard deviations. This image was generated through Python script

The average of k_3 is:

$$k_{3,mean} = -2.6 \cdot 10^{-5} \tag{3.36}$$

The standard deviation of k_3 is:

$$k_{3,\sigma} = 5.4 \cdot 10^{-6} \tag{3.37}$$

This parameter can be considered constant for the specific sensor used. It is correlated to the manufacturing process used and the defectivity of the device.

4 RESULTS AND DISCUSSION

Due to the large sensitivity of the fitting algorithm to μ, a Lorentzian fitting was carried out to the most linear set of data. Once the μ parameter was identified, the fitting computed the k_3 and K values.
The initial values of the resonance frequency λ and μ are close to their exact values, while k_3 and K can be deduced by vectorial fitting and square-low interpolation of previously fitted data.
A k_3 value was computed for a specific sensor:

$$k_3 = -2.6 \cdot 10^{-5} \pm 5.4 \cdot 10^{-6} \tag{4.1}$$

Multiple experiments can be carried out to other microGauge's sensors in order to characterize them through the extraction of their non-linear parameter.

4.1 LINEARITY'S BOUNDARY IDENTIFICATION

The objective of the fitting is to find the actuation potential limit between a linear and non-linear resonator. In this section, the procedure to compute this limit is described, with the assumptions and a real-data example.
The linearity limit is defined as the transition point between a monostable resonator to its bistable configuration. Algebraically, it means to find the transition point for a certain V_{outB} where Δ starts to have some negative values.
In figure 4.1 the value of Δ for $V_{outB} = 0.3\,V$ is reported.

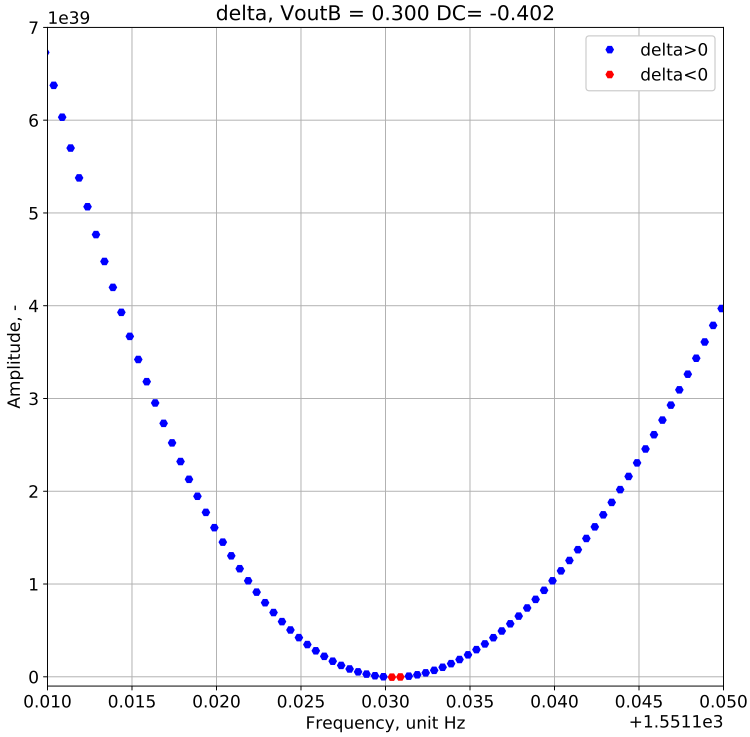

Figure 4.1: Delta values of a specific sensor, the red points in the middle of the figure represent the bi-stability of the device near its resonance frequency. This image was generated through Python script

4.2 LIMIT POTENTIAL

The automation procedure requires a consistent and defined actuation potential limit regardless of the fitting and the initial conditions. To check for consistency the algorithm for V_{limit} extraction was applied to several fittings.
The values of fitted parameters k_3 , λ , μ , K are inserted in the solution equation in order to find Δ

```
# This function performs the initial computations to deliver the Delta values
def deltafun(w,k3,mu,lb,K):
        a=float(9*k3**2/16)
        b=3*k3*(lb**2 - w**2)/2
        c=((lb**2 - w**2)**2+(mu**2)*w**2)
        d= -K**2
        p= c/a - b**2/(3*a**2)
        q= d/a - b*c/(3*a**2) + 2*b**3/(27*a**3)
```

```
    delta = q**2/4 + p**3/27
    return delta
```

Two loops are defined, one to increase K up to the non linearity condition, the other to decrease it until the resonator is linear:

```
# Those two loops change the K paramter in order to find
#   the minimum K for which Delta is totally positive
loopcheck=0
#Increase K until delta has some negative value
while np.all(delta > 0):
    loopcheck=+1
    if loopcheck > 1e4:
        raise ValueError('Error: K not found, infinite loop')
    K2=K2*1.5
    delta=deltafun(wdense,k3,mu,lb,K2)
loopcheck=0
#Decrease finely Delta until the optimal K is found
while np.any(delta < 0):
    loopcheck=+1
    if loopcheck > 1e4:
        raise ValueError('Error: K not found, infinite loop')
    K2=K2*0.999
    delta=deltafun(wdense,k3,mu,lb,K2)
```

The obtained value of Δ is shown in figure 4.2.

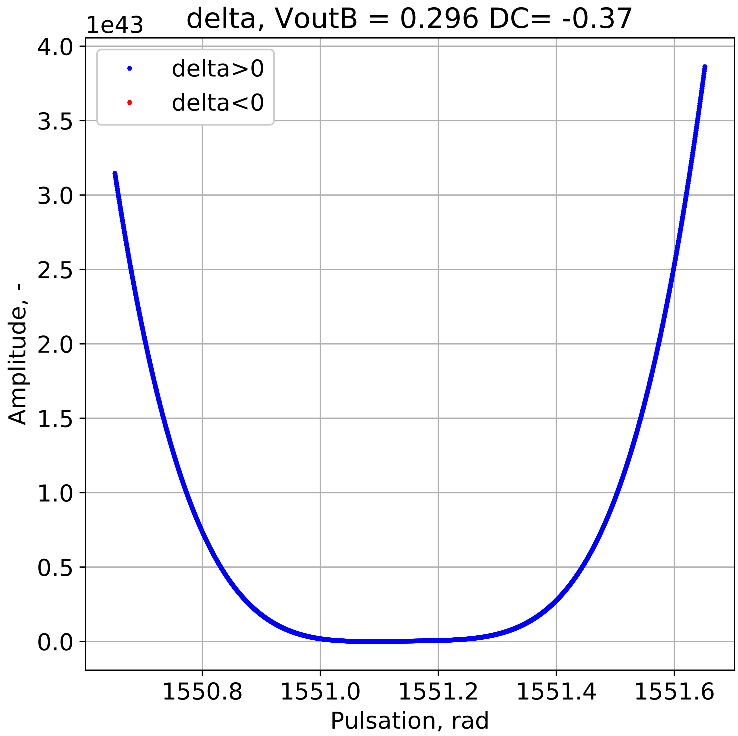

Figure 4.2: Delta prediction of the resonator when V_{outB} is at the limit of linearity. This image was generated through Python script

In the end it was found the V_{limit} value that define the limit between mono-stability and bi-stability through a simple quadratic proportionality with respect to K.

$$V_{limit} = V_{outB} \cdot \sqrt{\frac{K_{limit}}{K_{initial}}} \tag{4.2}$$

The average value of the limit actuation potential of a specific microGauge's device is:

$$V_{limit} = 0.303\,V \tag{4.3}$$

The standard deviation limit actuation potential is:

$$V_{limit,\sigma} = 0.0087\,V \tag{4.4}$$

5 CONCLUSION

In the closing stage of this thesis, a summary of the obtained results is presented.

ACTUATION LIMIT The obtained objective setpoint defines the limit boundary between mono-stability and bi-stability, hence the company is able to set the right actuation potential for every sensor. The calibration procedure does not depend on arbitrary evaluation, and thus it can be automated as stated in the introduction 1.

FITTING ROBUSTNESS The behaviour of the algorithm was tested through the computation of mock data, and consequently the mock data was fitted with different starting parameters. The converged results prove the robustness of the algorithm for certain variation of the initial parameters' conditions and set boundaries to their starting values.

EXPERIMENTAL DATA The algorithm is successfully applied to sensors' experimental data, with extraction of intrinsic parameters. Multiple experiments were carried out to check for the theory's consistency and the obtained results follow the expectations.

CHARACTERIZATION The k_3 parameter is related to the intrinsic non linearity of the device because it is related to the third coefficient of non linear Hooke's spring constant. It was made the assumption that k_3 is a constant and the outcomes in figure 3.15 bolster this statement.

CATEGORIZE The k_3 parameter is used also to categorize diverse sensors and to discriminate between several production processes.

FUTURE WORK

For future development the autonomous calibration procedure will be implemented using the presented algorithm. The automation of the process saves elaboration time and reduces the cost for production of new devices.
This algorithm is a starting point research for the elements affecting k_3. The company can be interested to minimize the above mentioned value in order to increase the actuation potential as much as possible.

A H.A.M.: MATHEMATICS

This appendix includes the mathematical fundamentals of the H.A.M. (homotopy analysis method) and gives an overview of its application with respect to harmonic resonator, according to the article [4, Non linear dynamics of MEMS/NEMS resonators].
In this chapter, you will find an overview of the Duffing equation, then a description of various sources of loss in a harmonic resonator, followed by the H.A.M. and concluded by a practical example of a harmonic oscillator actuated by two fixed electrodes.

A.1 DUFFING EQUATION

The Duffing equation is one of the most wide-spread model used to represent the non linear oscillation of a resonator.

$$\frac{d^2u}{d\tau^2} + \mu \cdot \frac{du}{d\tau} + \lambda^2 \cdot u + k_2 \cdot u^2 + k_3 \cdot u^3 = K \cdot \cos(w \cdot \tau) \tag{A.1}$$

- $u(\tau)$: non-dimensional modal displacement
- τ : non-dimensional time
- μ : viscous damping
- λ : natural frequency of the beam in its equilibrium configuration
- w : non-dimensional pulsation
- K : non-dimensional actuation amplitude
- k_2: second order non linear term
- k_3: third order non linear term

More details about this topic can be found in the following book: [9, The Duffing Equation: Nonlinear Oscillators and their Behaviour].
Shortly, a harmonic oscillator can exhibit a symmetric amplitude response, with respect to the actuation frequency thus, it can be considered as "Linear harmonic oscillator". In the cases where the amplitude response deviates from the symmetric shape, the oscillation magnitude will increase and the plot's peak would deviate from the centre towards one of the two sides. On top

of that, an hysteresis effect is observed for non linear oscillator.
The resonator, approaching the non linear region, will present one of the two following behaviour:

1. Hardening effect;
2. Softening effect;

In the first case, the plot's peak will shift towards the right side and in the second case it will lean towards the left side, as displayed in figures A.1a and A.1b.

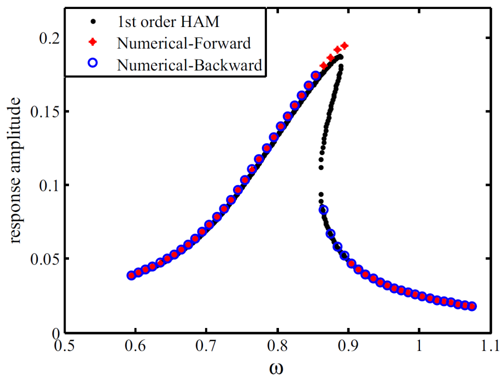

(a) Hardening behaviour of Duffing resonator

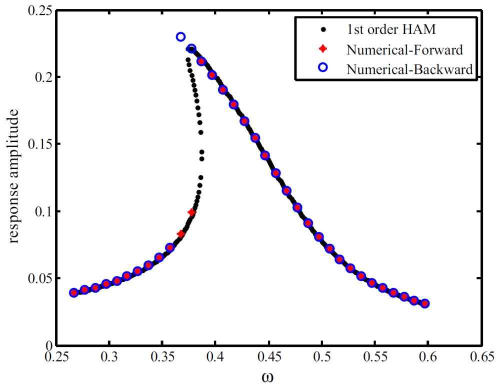

(b) Softening behaviour of Duffing resonator

Figure A.1: Distortion of the transfer function of a typical non linear resonator. The oscillator's peak lean towards one of the plot's sides. Images were extracted from the article [4, Non linear dynamics of MEMS/NEMS resonators] page 1919

These phenomena are related to the appearance of a non linear term (C_3) in the spring constant of the device. Thus, the resonator does not follow the Hooke's law, figure A.2.

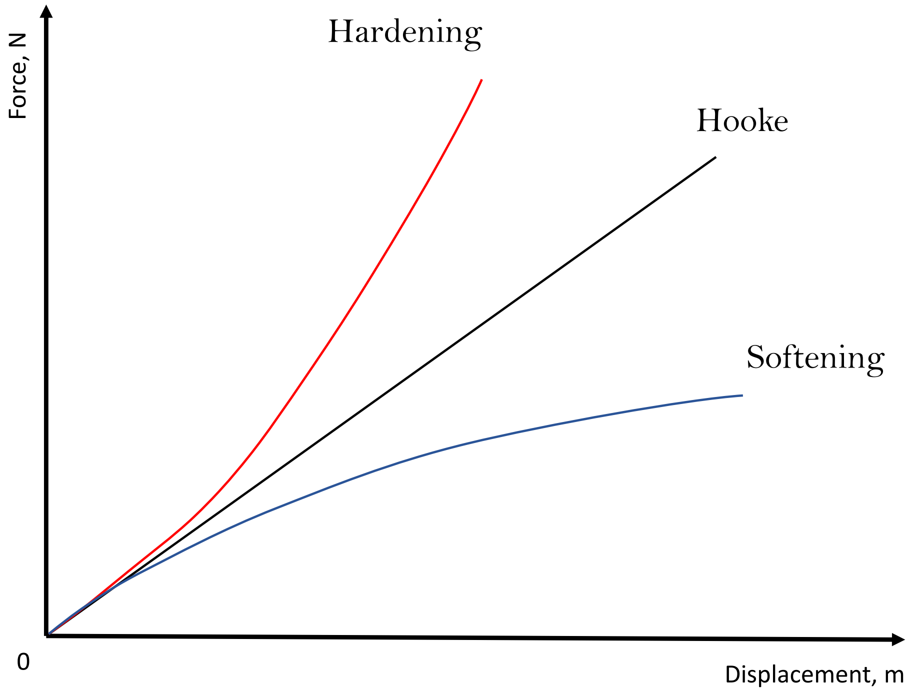

Figure A.2: This figure describes the deviation from the Hooke's law. The red curve represents an hardening type spring, the blue curve a softening type and the black line the Hooke's law. This image was generated through Microsoft PowerPoint

The non linear spring is described by the following equation A.2.

$$F = C_1 z + C_3 z^3 \tag{A.2}$$

Where F is the force applied, C_1 the linear spring constant, C_3 the first order approximation term of the non linear spring constant and z the displacement.
In the Hooke's law only the C_1 term exist. If the spring presents some non linearity, then the C_3 term appear as a Taylor expansion of the spring constant. In the case $C_3 > 0$ the device has the hardening effect, because the same displacement requires higher force, on the other hand in the case $C_3 < 0$ the device has the softening effect, and thus the same displacement requires less force.
The equation A.2 can be translated in the force equation of an oscillator, as shown in the equation A.3.

$$\frac{\mathrm{d}^2 z}{\mathrm{d}t^2} + \nu \cdot \frac{\mathrm{d}z}{\mathrm{d}t} + C_1 \cdot z + C_3 \cdot z^3 = F \cdot \cos(w \cdot t) \tag{A.3}$$

Where:

- z : displacement

- t : time
- ν : viscous damping coefficient
- C_1 : linear spring constant
- C_3 : first order approximation term of the non linear spring constant
- w : pulsation
- F : force

By normalizing the values and dividing by the mass the Duffing equation is obtained A.1. The terms λ and k_3 appear as:

$$\lambda = \frac{1}{2\pi}\sqrt{\frac{C_1}{m}} \tag{A.4}$$

$$\sqrt{k_3} = \frac{1}{2\pi}\sqrt{\frac{C_3}{m}} \tag{A.5}$$

The k_3 parameter is related to C_3, and thus it is a constant representing the intrinsic non linearity of the oscillator.
Historically, the Duffing equation was resolved through non-perturbation techniques [10, An approximate solution technique depending on an artificial parameter: A special example]. Such techniques use small parameters assumption that would not be reliable in case of high non linear problems since it would lose its physical meaning.
Meanwhile, the H.A.M. does not depend on any small parameter assumption and it can guarantee the convergence of a numerical solution through an artificial parameter: c_0 [4, Non linear dynamics of MEMS/NEMS resonators].

A.2 H.A.M. CONVERGENCE

H.A.M. is intended to derive a solution analytically or semi-analytically, for the non linear response of the forced vibrations in a typical MEMS resonator.
It is supposed that the solution has the following form:

$$u(\tau) = \delta + \sum_{k=1}^{\infty}\left(U_k \cdot \exp(ikw\tau) + \overline{U}_k \cdot \exp(-ikw\tau)\right) \tag{A.6}$$

The parameters of equation A.6 are:

- δ: long-time average of the harmonic response
- U_k, $\overline{U}_k$: complex conjugate constants

To express a continuous evolution from an initial estimate $\phi(0)$ to the final solution, it is declared an embedding parameter $p \in [0, 1]$ and a variation $\phi(\tau, p)$ so that:

$$\phi(\tau, p) : \Re^{+} x [0, 1] \rightarrow \Re \tag{A.7}$$

The function $\phi(\tau, p)$ displays a continuous evolution proceeding from the initial estimate, when $p = 0$, up to the final solution:

$$\phi(\tau, 1) = u(\tau) \quad \text{Final solution} \tag{A.8}$$

As p varies from 0 to 1, it is possible to replace $u(\tau)$ of equation A.1 with the variation $\phi(\tau, p)$, thus, it is possible to construct the non linear operator $\Psi[\phi(\tau, p), \tau]$.

$$\Psi[\phi(\tau, p), \tau] = \frac{\partial^2 \phi}{\partial \tau^2} + \mu \frac{\partial \phi}{\partial \tau} + \lambda^2 \cdot \phi + k_2 \cdot \phi^2 + k_3 \cdot \phi^3 - K \cdot \cos(w \cdot \tau) \tag{A.9}$$

The equation A.9 represents the residual error of the variation with respect to the exact solution. The expected solution have to satisfy a proper linear-differential operator:

$$\Gamma[\phi(\tau, p)] = \frac{\partial^2 \phi}{\partial \tau^2} + w^2 \cdot \phi(\tau, p) \tag{A.10}$$

Thus, there are all the elements to construct the *Zero-order deformation equation* according to the article: [4, Non linear dynamics of MEMS/NEMS resonators]:

$$(1 - p) \cdot \Gamma[\phi(\tau, p) - u_0(\tau)] = c_0 \cdot p \cdot \Psi[\phi(\tau, p)] \tag{A.11}$$

The parameters of equation A.11 are reported:

- c_0: convergence control parameter
- u_0: initial estimate of modal displacement

According to the author of the H.A.M. S. Liao [1, Advances in the homotopy analysis method], the c_0 parameter does not have any physical solution and it can be adjusted to make algebraic series always convergent.
The initial estimate of the modal displacement can be expressed as equation A.12:

$$u_0(\tau) = \delta_0 + \sum_{k=1}^{\infty} \left(U_{0k} \cdot \exp(ikw\tau) + \overline{U}_{0k} \cdot \exp(-ikw\tau)\right) \tag{A.12}$$

The definition of the variation $\phi(\tau, p)$ is a convergent series in p, with $u_k(\tau)$ as the deformation derivatives, expressed in A.14.

$$\phi(\tau, p) = \sum_{k=0}^{\infty} \left(u_k(\tau) \cdot p^k\right) \tag{A.13}$$

$$u_k(\tau) = \frac{1}{k!} \frac{\partial^k \phi(\tau, p)}{\partial p^k}\bigg|_{p=0} \tag{A.14}$$

A.3 HIGHER-ORDER DEFORMATION EQUATION

Through an iterative approach it is possible to solve the following k-th order deformation equation for $u_k(\tau)$ until the ordering number reduces the approximation's residuals to the desired level.

$$\Gamma\left[u_k(\tau) - \chi_k \cdot u_{k-1}(\tau)\right] = c_0 \cdot R_k(\tau) \tag{A.15}$$

with:

$$\chi_k = \begin{cases} 0, & \text{if } k \leq 1 \\ 1, & \text{if } k > 1 \end{cases} \tag{A.16}$$

$$R_k(\tau) = \frac{1}{(k-1)!} \frac{\partial^{k-1}}{\partial p^{k-1}} \Psi\left[\phi\left(\tau, p\right), \tau\right]\Big|_{p=0} \tag{A.17}$$

Through this method it is possible to compute the next k-th solution starting from the previous step.
The final solution of equation A.1 is found by setting $p = 1$ in the obtained series solution.

A.4 FIRST ORDER H.A.M APPROXIMATION

Suppose $u_0(\tau)$ is consistent with the rule of solutions of equation A.6, then the initial estimate is:

$$u_0(\tau) = \delta_0 + U_{0k} \cdot \exp(ikw\tau) + \overline{U}_{0k} \cdot \exp(-ikw\tau) \tag{A.18}$$

The first order-deformation equation is reckoned through the initial estimate and the equations A.15, A.16, A.17.

$$\frac{\partial^2 u_1(\tau)}{\partial \tau^2} + w^2 \cdot u_1(\tau) = c_0 \cdot \Psi\left[u_0\left(\tau\right), \tau\right] \tag{A.19}$$

The formula A.19 must have bounded solution so it is necessary to eliminate the secular and constant terms by setting them to zero.
Zeroing secular terms:

$$c_0 \cdot f_1\left(U, \overline{U}, \delta\right) = 0 \tag{A.20}$$

Zeroing constant terms:

$$c_0 \cdot g_1\left(U, \overline{U}, \delta\right) = 0 \tag{A.21}$$

The coefficients U, $\overline{U}$ are defined by the amplitude z and the phase shift b of the response signal.

$$\begin{aligned} U &= \frac{1}{2} z e^{i \cdot b} \\ \overline{U} &= \frac{1}{2} z e^{-i \cdot b} \end{aligned} \tag{A.22}$$

Introducing them into equations A.20 and A.21 it is possible to obtain the long-time average constant and the response frequency.

$$\delta = \frac{-z^2 \cdot k_2}{2\lambda^2 + 3z^2 \cdot k_3} \tag{A.23}$$

$$\left(2k_2 \cdot \delta \cdot z + \frac{3}{4}k_3 \cdot z^3 + \left(\lambda^2 - w^2\right) \cdot z\right)^2 + (\mu \cdot w \cdot z)^2 = K^2 \tag{A.24}$$

In the equations A.23 and A.24 all the terms δ^2 and its higher power are neglected. In the latter equation, A.24 it is possible to compute the amplitude value z knowing all the parameters of the Duffing equation A.1.
A typical amplitude response of a non linear resonator using H.A.M approach is displayed in the figure A.1a, in which the H.A.M. numerical solution is printed with black dots and it is compared with a numerical-forward approach (red diamonds) and a numerical-backward approach (blue rings).
It is possible to notice that the H.A.M calculation is more consistent and can give an approximate solution in one sweeping computation while other techniques require a forward and backward run.

A.5 STRAIGHT BEAM WITH DOUBLE CLAMPED ELECTRODES

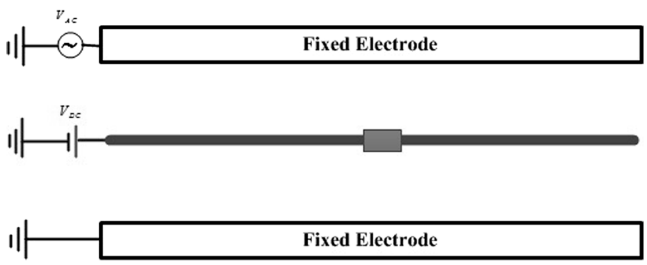

Figure A.3: Schematic of a straight beam with double clamped electrodes, a DC potential is applied to the beam while an oscillating actuation potential is applied to the top electrode. Images were extracted from the article [4, Non linear dynamics of MEMS/NEMS resonators] pag. 1919

Figure A.3 shows a bounded beam between two electrodes, where the top electrode imposes an alternating potential, while a direct voltage is applied on the beam.
From the article [11, Chaos prediction in MEMS-NEMS resonators] the equation of the transverse motion of a lumped system with a single degree of freedom is extracted.

$$\frac{\partial^2 \chi}{\partial \tau^2} + \mu\frac{\partial \chi}{\partial \tau} + \chi + \beta \cdot \chi^3 = \gamma \cdot \left[\frac{1}{(1-\chi)^2} - \frac{1}{(1+\chi)^2}\right] + \frac{A}{(1-\chi)^2}\sin(w \cdot \tau) \tag{A.25}$$

The parameters are defined as:

- χ: non dimensional lateral displacement
- τ: non dimensional time
- w: non dimensional actuation frequency
- μ: non dimensional viscous damping coefficient
- β: stretching parameter
- γ: DC potential parameter

Through a MacLaurin series the non linear terms χ near the origin is expanded up to the 3° order. Neglecting the coefficients of the harmonic terms, this yields:

$$\frac{\partial^2 \chi}{\partial \tau^2} + \mu \frac{\partial \chi}{\partial \tau} + \lambda^2 \cdot \chi + k_3 \cdot \chi^3 = K \sin(w \cdot \tau) \tag{A.26}$$

in which:

$$\lambda^2 = 1 - 4 \cdot \gamma \tag{A.27}$$

$$k_3 = \beta - 8 \cdot \gamma \tag{A.28}$$

$$K = A \tag{A.29}$$

For the equation A.26 the constrain is that the origin has to be a stable point thus, $\gamma < \frac{1}{4}$.
By using this function, it is possible to prove experimentally the validity of the H.A.M. solution, confronting the amplitude response with the equation A.24 yielding:

$$\left(\frac{3}{4} k_3 \cdot z^3 + \left(\lambda^2 - w^2\right) \cdot z\right)^2 + (\mu \cdot w \cdot z)^2 = K^2 \tag{A.30}$$

B MICROGAUGE PROFITS

In this chapter the average profit that the company *microGauge AG* gained introducing the automated procedure is computed.
The average salary of an engineer per hour is $Q_{eng} = 50.00\,\texttt{CHF/h}$, in the present state of the organization, a microGauge's specialist is calibrating manually every new sensors.
The mean time to take a point in a frequency sweep is $60\,s$ and usually there are 14 points in a frequency sweep.
The specialist uses in average 20 frequency sweeps to calibrate properly a device, thus it is needed 280 minutes overall.
This new automated procedure needs only 1 or 2 frequency sweeps to find the bi-stability limit, thus it takes in the worst-case scenario 28 minutes.
The time saved using the algorithm is:

$$t_{saving} = t_{operator} - t_{algorithm} = 252\,min \tag{B.1}$$

The equivalent salary saved by the company, for only one calibrated device, is:

$$C_{saved} = t_{saving} \cdot Q_{eng} = 210\,\texttt{CHF} \tag{B.2}$$

Moreover, it is pointed out that the specialist can calibrate at the same time up to 8 sensors together, while the automated procedure does not have any parallelisation limit.

LIST OF SYMBOLS

E.T.H.	Swiss Federal Institute of Technology
H.A.M.	homotopy analysis method
AG	Public limited company
F.W.H.M.	full width at half maximum
$u(\tau)$	non-dimensional modal displacement
τ	non-dimensional time
μ	viscous damping
λ	natural frequency of the beam in its equilibrium configuration
w	actuation frequency
K	non-dimensional actuation amplitude
k_2	second order non linear term
k_3	third order non linear term
F	force
C_1	linear spring constant
C_3	first order approximation term of the non linear spring constant
z	displacement
ϱ	harmonic oscillator phase
w_{res}	harmonic oscillator resonance frequency
A	harmonic oscillator amplitude
σ	harmonic oscillator half frequency width
$V(u)$	potential function of Duffing's equation
δ	long-time average of the harmonic response
U_k, $\overline{U}_k$	complex conjugate constants of the homotopy solution
$u_0(\tau)$	initial estimate of homotopy solution
$\Re$	real numbers
Ψ	non linear operator
Γ	linear operator
c_0	convergence control parameter
y	root square of amplitude response
a	first coefficient of third order polynomial
b	second coefficient of third order polynomial
c	third coefficient of third order polynomial
d	fourth coefficient of third order polynomial
x	shifted root square of amplitude response by $\frac{-b}{3a}$
Δ	discriminant of cubic equation
V_{AC}	alternate applied potential
V_{DC}	direct applied potential

$z_{estimated}$	amplitude value computed with estimated parameters
$k_{3,\,estimated}$	initial non linear coefficient
$k_{3,\,mean}$	average of the non linear coefficient
$k_{3,\,\sigma}$	standard deviation of the non linear coefficient
$\mu_{estimated}$	initial viscous coefficient
$K_{estimated}$	initial amplitude coefficient
λ_{max}	upper boundary of resonance frequency
λ_{min}	lower boundary of resonance frequency
$k_{3,\,max}$	upper boundary of non linear term
$k_{3,\,min}$	lower boundary of non linear term
μ_{max}	upper boundary of viscosity
μ_{min}	lower boundary of viscosity
K_{max}	upper boundary of actuation parameter
K_{min}	lower boundary of actuation parameter
V_{outB}	experimental applied potential
V_{limit}	limit potential at bi-stability
$V_{limit,\,\sigma}$	standard deviation of limit potential at bi-stability
K_{limit}	actuation coefficient at bi-stability
$K_{initial}$	actuation coefficient extracted from experiment
Q_{eng}	estimation of the average salary of an engineer per hour
t_{saving}	time difference between the algorithm and an human operator
C_{saved}	gross profit of the company

ACKNOWLEDGEMENTS

I would like to say thanks to the microGauge company and the team for the good time spent together and the challenges that we overcame. In particular I extend my gratitude to *Christian Peters* for supervising me and the support given throughout the project.
I would also like to say thanks to my family for their patience and support as it is because of them I could study and live abroad.
Finally, I would like to thanks in particular *Harmina Vejayan* because of the moral support and the sweet company that she offered to me in this period.

BIBLIOGRAPHY

[1] S. Liao, *Advances in the Homotopy Analysis Method*. 2013.

[2] M. Aubry, H. J. Baues, S. Halperin, and J.-M. J.-M. Lemaire, *Homotopy theory and models : based on lectures held at a DMV Seminar in Blaubeuren by H.J. Baues, S. Halperin, and J.-M. Lemaire*. Birkhäuser Basel, 1995.

[3] W. Ewald, *From Kant to Hilbert : a source book in the foundations of mathematics*. Clarendon Press, 1996.

[4] F. Tajaddodianfar, M. R. H. Yazdi, and H. N. Pishkenari, "Nonlinear dynamics of MEMS/NEMS resonators: analytical solution by the homotopy analysis method," *Microsystem Technologies*, vol. 23, no. 6, pp. 1913–1926, 2017.

[5] *The Duffing Oscillator*, pp. 157–184. Berlin, Heidelberg: Springer Berlin Heidelberg, 2008.

[6] M. Fierz, "Cardano's Life and Writings," in *Girolamo Cardano*, pp. 1–36, Boston, MA: Birkhäuser Boston, 1983.

[7] M. Newville, T. Stensitzki, D. B. Allen, and A. Ingargiola, "LMFIT: Non-Linear Least-Square Minimization and Curve-Fitting for Python," sep 2014.

[8] M. Newville, T. Stensitzki, D. B. Allen, and A. Ingargiola, "LMFIT: Non-Linear Least-Square Minimization and Curve-Fitting for Python," sep 2014.

[9] I. Kovacic and M. J. M. J. Brennan, *The Duffing equation : nonlinear oscillators and their phenomena*. Wiley, 2011.

[10] A. Hatcher, "An approximate solution technique depending on an artificial parameter: A special example," *Communications in Nonlinear Science and Numerical Simulation*, vol. 3, pp. 92–97, jun 1998.

[11] E. Maani Miandoab, H. N. Pishkenari, A. Yousefi-Koma, and F. Tajaddodianfar, "Chaos prediction in MEMS-NEMS resonators," *International Journal of Engineering Science*, vol. 82, pp. 74–83, sep 2014.